Full title: Antagonistic paralogs control a switch between growth and pathogen resistance in *C. elegans*

Short title: A switch for *C. elegans* resistance to diverse natural pathogens

Kirthi C. Reddy*, Tal Dror*, Ryan S. Underwood*, Guled A. Osman#, Christopher A. Desjardins^, Christina A. Cuomo^, Michalis Barkoulas#, and Emily R. Troemel*

*Division of Biological Sciences, University of California, San Diego, La Jolla, CA 92093 USA

^Infectious Disease and Microbiome Program, Broad Institute, Cambridge MA 02142 USA

Department of Life Sciences, Imperial College, London SW7 2AZ, UK

Lead contact: Emily Troemel, 9500 Gilman Dr #0349, La Jolla, CA 92093, USA

etroemel@ucsd.edu

Abstract

Immune genes are under intense pressure from pathogens, which cause these genes to diversify over evolutionary time and become species-specific. Through a forward genetic screen we recently described a *C. elegans*-specific gene called *pals-22* to be a repressor of "Intracellular Pathogen Response" or IPR genes. Here we describe *pals-25*, which, like *pals-22*, is a species-specific gene of unknown biochemical function. We identified *pals-25* in a screen for suppression of *pals-22* mutant phenotypes and found that mutations in *pals-25* suppress all known phenotypes caused by mutations in *pals-22*. These phenotypes include increased IPR gene expression, thermotolerance, and immunity against natural pathogens. Mutations in *pals-25* also reverse the reduced lifespan and slowed growth of *pals-22* mutants. Transcriptome analysis indicates that *pals-22* and *pals-25* control expression of genes induced not only by natural pathogens of the intestine, but also by natural pathogens of the epidermis. Indeed, in an independent forward genetic screen we identified *pals-22* as a repressor and *pals-25* as an activator of epidermal defense gene expression. These phenotypic and evolutionary features of *pals-22* and *pals-25* are strikingly similar to species-specific R gene pairs in plants that control immunity against co-evolved pathogens.

Introduction

Evolutionarily ancient genes control core processes in diverse organisms. For example, the >500 million-year-old Hox gene cluster is required for establishing body plan polarity in animals as diverse as worms, flies and humans [1]. However, evolutionarily young genes can also play key roles in development. For example, the *Drosophila* Umbrea gene only evolved within the *Drosophila* lineage in the last 15 million years but is

44 essential for chromosome segregation in *Drosophila melanogaster* [2]. In general, the
45 functions of evolutionarily young genes are less well understood than the function of
46 evolutionarily ancient genes.
47
48 New genes can arise through gene duplication and diversification [3]. Extensive gene
49 duplication can lead to large, expanded gene families, which appear 'species-specific' if
50 there is significant diversification away from the ancestral gene. The function of species-
51 specific genes can provide insight into the pressures imposed upon organisms in their
52 recent evolutionary past. Pathogen infection imposes some of the strongest selective
53 pressure on organisms, and accordingly, many species-specific, expanded gene families
54 are involved in immunity. One example is the family of mouse Naip genes, which encode
55 sensor proteins in the inflammasome that detect bacteria to trigger cytokine release and
56 cell death [4]. Another example is the plant R genes, which detect virulence factors from
57 co-evolved pathogens to activate effector-triggered immunity [5]. Interestingly, a growing
58 theme in plant R genes is that they can function as opposing gene pairs, with one R
59 gene promoting host defense and the other R gene inhibiting host defense. Of note, both
60 the Naip and R genes were identified through unbiased forward genetic screens for
61 immune genes.
62
63 Recently, we described a forward genetic screen in *C. elegans* for genes that regulate
64 the transcriptional response to natural intracellular pathogens [6]. From this screen we
65 identified a *C. elegans*-specific gene called *pals-22* that regulates expression of
66 Intracellular Pathogen Response or IPR genes. Interestingly, we found that *pals-22* also
67 regulates proteostasis, potentially through ubiquitin ligase activity (see below). The '*pals'*
68 signature stands for <u>p</u>rotein containing <u>ALS</u>2CR12 signature, which is found in the single

69 *pals* gene in humans called ALS2CR12. A genome-wide association study implicated
70 ALS2CR12 in amyotrophic lateral sclerosis (ALS) [7], although this gene has no known
71 role in ALS, and its biological function is unknown. The *pals* gene family has only a
72 single member each in the mouse and human genomes, but is substantially expanded in
73 *Caenorhabditis* genomes: *C. elegans* has 39 *pals* genes; *C. remanei* has 18 *pals* genes;
74 *C. brenneri* has 8 *pals* genes; and *C. briggsae* has 8 *pals* genes [8].
75
76 *pals-22* mutants have several striking phenotypes in *C. elegans*. First, *pals-22* mutants
77 have constitutive expression of several IPR genes including the cullin gene *cul-6*, which
78 is predicted to encode a component of a Cullin-Ring Ligase complex. Second, *pals-22*
79 mutants have increased tolerance of proteotoxic stressors, and this increased tolerance
80 requires the wild-type function of *cul-6*. Third, *pals-22* mutants have less robust health in
81 the absence of stressors. In particular, they have slowed development and shorter
82 lifespans compared to wild-type animals. Fourth, as shown by another group who
83 identified *pals-22* in an independent forward genetic screen, *pals-22* mutants have
84 increased transgene silencing, and increased RNA interference (RNAi) against
85 exogenous RNA [8]. Thus, loss-of-function mutations in *pals-22* appear to broadly
86 reprogram the physiology of *C. elegans*.
87
88 Here we describe a forward genetic screen for suppressors of *pals-22* and identify
89 another *pals* gene called *pals-25*. Interestingly, although it appears that *pals-25* and
90 *pals-22* are in an operon together, these two genes function antagonistically and direct
91 opposing phenotypes. We show that mutations in *pals-25* strongly suppress all the
92 physiological phenotypes seen in *pals-22* mutants, including IPR gene expression,
93 stress resistance, lifespan, development and transgene silencing. Furthermore, we find

that *pals-22* mutants have increased resistance against natural intracellular pathogens, like the microsporidian species *Nematocida parisii* and the Orsay virus. This increased resistance is suppressed by mutations in *pals-25*. Also, we use RNA-seq analysis to show that the *pals-22/pals-25* gene pair (hereafter referred to as *pals-22/25*) regulate expression of a majority of the genes induced by natural pathogens of the intestine and find that most of these genes are also induced by blockade of the proteasome. Interestingly, we observe that *pals-22* and *pals-25* also regulate expression of genes induced by natural eukaryotic pathogens infecting through the epidermis. Indeed, in an independent forward genetic screen to find regulators of epidermal defense gene expression we identified additional mutant alleles of *pals-22* and *pals-25*. In summary, the species-specific *pals-22/25* gene pair control an entire physiological program that balances growth with increased proteostasis capacity and resistance against diverse natural pathogens.

Results

pals-25 is required for increased IPR gene expression in *pals-22* mutants

Previously we found that wild-type *pals-22* represses expression of IPR genes: *pals-22* mutants have constitutive expression of several IPR genes including *pals-5* [6]. A transcriptional reporter consisting of the 1273 bp upstream region of *pals-5* fused to GFP, *pals-5p::GFP,* is a reliable marker of IPR gene expression [9] and exhibits strong GFP expression in a *pals-22* mutant background [6] (Fig 1A-C). To find positive regulators of IPR gene expression, we mutagenized *pals-22*; *pals-5p::GFP* strains and screened for loss of GFP expression in F2 animals. From one screen in the *pals-22(jy1)* mutant background and one screen in the *pals-22(jy3)* mutant background we screened a total of ~23,000 haploid genomes and found eight independent mutant alleles that

119 almost entirely reverse the increased *pals-5p::GFP* expression back to wild-type levels in
120 *pals-22* mutants (Fig 1A-F). All of these alleles are recessive, segregate in Mendelian
121 ratios, and fail to complement each other. These results suggest they all have loss-of-
122 function mutations in the same gene.
123
124 We used whole-genome sequencing of two mutant strains (*jy9* and *jy100*) to identify the
125 causative alleles [10] and found predicted loss of function mutations in *pals-25* in both
126 strains. Further sequencing identified *pals-25* mutations in the remaining six mutant
127 strains (Fig 1G, S1 Table). *pals-25* appears to be in an operon just downstream of *pals-*
128 *22*, and while these two genes are paralogs, they share limited sequence similarity, with
129 no significant similarity on the DNA level and only 19.4% identity on the amino acid level.
130 Of note, neither *pals-22* nor *pals-25* have obvious orthologs in other *Caenorhabditis*
131 species, and thus appear to be specific to *C. elegans* [8]. To further confirm that *pals-25*
132 regulates *pals-5p::GFP* gene expression in *pals-22* mutants, we performed RNAi against
133 *pals-25* in a *pals-22*; *pals-5p::GFP* strain. As expected, we found lowered expression of
134 *pals-5p::GFP* (Fig 1H, S2 Fig), indicating that wild-type *pals-25* is required for the
135 increased expression of *pals-5p::GFP* seen in a *pals-22* mutant background.
136
137 These observations suggest that *pals-25* acts downstream of *pals-22* to activate mRNA
138 expression of IPR genes. To test this hypothesis, we used qRT-PCR to measure levels
139 of endogenous mRNA in *pals-22 pals-25* mutants compared to *pals-22* mutants and
140 wild-type animals (Fig 2A). We analyzed mRNA levels of *pals-5*, as well as seven other
141 IPR genes including nematode-specific genes of unknown function (F26F2.1, F26F2.3,
142 and F26F2.4), and predicted ubiquitin ligase components *skr-3, skr-4, skr-5* and *cul-6*.
143 Here we found that mutations in *pals-25* reverse the elevated mRNA levels of all eight of

144 these IPR genes in a *pals-22* mutant background back to near wild-type levels.
145 Importantly, a non-IPR gene, *skr-1*, is not affected by mutations in *pals-22* or *pals-25*.
146 These results indicate that in a *pals-22* mutant background, wild-type *pals-25* activates
147 IPR gene expression.
148
149 Previous analysis indicated that *pals-22* is broadly expressed in several tissues in the
150 animal, including the intestine and the epidermis [6, 8]. Similarly, we found that *pals-25* is
151 broadly expressed. Using a fosmid containing *pals-25* with endogenous *cis* regulatory
152 control and tagged at the C terminus with GFP and 3xFLAG [11], we observed PALS-
153 25::GFP expression throughout the animal, including expression in the neurons,
154 epidermis, and intestine (S2B Fig). We did not see any change in PALS-25::GFP
155 expression after *pals-22* RNAi treatment (S2C Fig).
156
157 **IPR genes are induced by infection and by proteasome blockade in *pals-22 pals-***
158 ***25* mutants**
159 As *pals-25* is required to activate IPR gene expression in a *pals-22* mutant background,
160 we wondered whether *pals-25* was required for inducing IPR gene expression in
161 response to external triggers. We originally identified IPR genes because of their
162 induction by *N. parisii* infection [6, 9], which is an intracellular pathogen in the
163 Microsporidia phylum that invades and undergoes its entire replicative life cycle inside *C.*
164 *elegans* intestinal cells [12]. We therefore infected animals with *N. parisii* and compared
165 induction of IPR genes in *pals-22 pals-25* mutants and wild-type animals at 4 hours (Fig
166 2B). Here we found similar levels of IPR gene induction in *pals-22 pals-25* and wild-type
167 animals, suggesting that *pals-22*/*25* regulate expression of IPR genes in parallel to
168 infection. Next, we examined the role of *pals-22*/*25* in the transcriptional response to

169 proteasome blockade, which is another trigger of IPR gene expression [9] (Fig 2C). We
170 used bortezomib, which is a small molecule inhibitor of the 26S proteasome. Here again,
171 we found that bortezomib treatment induced IPR gene expression in *pals-22 pals-25*
172 mutants at levels similar to wild-type animals. Therefore *pals-22/25* appear to regulate
173 IPR gene expression in parallel to infection and proteasomal stress.
174
175 ***pals-25* mutations reverse multiple physiological phenotypes caused by *pals-22***
176 **mutations**
177 *pals-22* mutants have several striking physiological phenotypes, including slowed growth
178 and shorter lifespans, as well as increased resistance to proteotoxic stress like heat
179 shock [6]. Therefore, we investigated whether mutations in *pals-25* suppress these
180 phenotypes of *pals-22* mutants. First, we investigated developmental rate by measuring
181 the fraction of animals that reach the fourth larval (L4) stage by 48 hours after
182 embryogenesis. Nearly all wild-type animals are L4 at this timepoint, whereas less than
183 20% of *pals-22* mutants are L4 (Fig 3A). We found that mutations in *pals-25* completely
184 reverse this delayed development of *pals-22* mutants, with nearly all *pals-22 pals-25*
185 mutants reaching the L4 stage by 48 hours (Fig 3A). Next, we analyzed lifespan, as
186 previous work showed that *pals-22* mutants have a significantly shortened lifespan
187 compared to wild-type animals [6, 8]. Here again we found that *pals-25* mutations
188 reversed this effect, with *pals-22 pals-25* mutants having lifespans comparable to wild-
189 type animals (Fig 3B, S3A-B Fig). Next, we investigated the effect of *pals-25* mutations
190 on the thermotolerance capacity of *pals-22* mutants, which is greatly enhanced
191 compared to wild-type animals. We found that *pals-22 pals-25* double mutants have
192 survival after heat shock at levels similar to wild-type animals (Fig 3C, S3C-D Fig),
193 indicating that *pals-25* is required for the enhanced thermotolerance of *pals-22* mutants.

194 Thus, these results show that in a *pals-22* mutant background, wild-type *pals-25* is
195 required to delay development, shorten lifespan and enhance thermotolerance.
196
197 Previous work from the Hobert lab identified *pals-22* in a screen for regulators of reporter
198 gene expression in neurons [8]. They found that mutations in *pals-22* led to decreased
199 levels of GFP reporter expression in neurons and other tissues, and wild-type *pals-22*
200 thus acts as an 'anti-silencing' factor of multi-copy transgene expression. Therefore, we
201 analyzed the effects of *pals-25* mutations on transgene silencing in *pals-22* mutants.
202 Here we found that *pals-25* mutations reverse the enhanced silencing of a neuronally
203 expressed GFP transgene in *pals-22* mutants (Fig 3D-I), indicating that wild-type *pals-25*
204 activity is required to silence expression from multi-copy transgenes in a *pals-22* mutant
205 background. Of note, previous work found that a *pals-25* mutation alone does not affect
206 transgene silencing [8]. In summary, mutations in *pals-25* appear to fully reverse all
207 previously described phenotypes of *pals-22* mutants.
208
209 ***pals-22* mutants have immunity against coevolved intestinal pathogens of the**
210 **intestine, which is suppressed by *pals-25* mutations**
211 In addition to the previously described phenotypes of *pals-22* mentioned above, we
212 analyzed resistance of these mutants to intracellular infection. First we analyzed the
213 resistance of *pals-22* mutants to *N. parisii* infection. We fed animals a defined dose of
214 microsporidia spores and measured pathogen load inside intestinal cells. We analyzed
215 pathogen load at 30 hours post infection (hpi), when *N. parisii* is growing intracellularly in
216 the replicative meront stage, and found greatly lowered pathogen load in *pals-22*
217 mutants compared to wild-type animals (Fig 4A-F). We then tested *pals-22 pals-25*
218 double mutants and found these animals to have resistance comparable to wild-type.

219 One explanation for the altered levels of *N. parisii* observed in the intestines of *pals-22*
220 mutant animals is that these mutants have lowered feeding or accumulation of pathogen
221 in the intestine, and thus simply have a lower exposure to *N. parisii*. To address this
222 concern, we added fluorescent beads to our *N. parisii* infection assay and measured
223 accumulation in the intestinal lumen. Here we found that *pals-22* mutants and *pals-22*
224 *pals-25* double mutants accumulated fluorescent beads at comparable levels to wild-type
225 animals (S4A Fig), suggesting that their pathogen resistance to *N. parisii* is not simply
226 due to lowered exposure to the pathogen in the intestinal lumen. As a positive control in
227 this assay we tested *eat-2(ad465)* mutants and found that they had reduced fluorescent
228 bead accumulation, consistent with their previously characterized feeding defect [13].
229 Altogether, these results indicate that *pals-22* and *pals-25* regulate resistance to
230 infection by microsporidia.
231
232 We also investigated resistance of *pals-22* mutants and *pals-22 pals-25* double mutants
233 to other pathogens. First, we measured resistance to infection by the Orsay virus. Like
234 *N. parisii*, Orsay virus is a natural pathogen of *C. elegans,* and replicates inside of *C.*
235 *elegans* intestinal cells [14]. We used FISH staining of Orsay viral RNA to quantify the
236 fraction of worms infected at 18 hpi. Here we found that *pals-22* mutants had significantly
237 decreased viral load when compared to wild-type animals (Fig 4G-L). This lowered viral
238 infection in *pals-22* mutants was fully reversed in *pals-22 pals-25* mutants back to wild-
239 type levels. Importantly, we confirmed that *pals-22* and *pals-22 pals-25* mutants do not
240 have altered fluorescent bead accumulation in the intestine compared to wild-type
241 animals in the presence of virus (S4B Fig), indicating that their lowered viral load is not
242 likely due to lowered exposure to the virus.
243

244 Interestingly, we found that *pals-22* mutants did not have reduced pathogen loads when
245 infected with the Gram-negative bacterial pathogen *Pseudomonas aeruginosa* (clinical
246 isolate PA14) (Fig 4M). In fact, these mutants had increased pathogen load, which was
247 suppressed by mutations in *pals-25*. To our knowledge *P. aeruginosa* species are not
248 common pathogens of nematodes in the wild, although under laboratory conditions, *P.*
249 *aeruginosa* PA14 does accumulate in the *C. elegans* intestinal lumen and causes a
250 lethal infection [15]. In summary *pals-22* mutants have increased resistance to natural
251 pathogens of the intestine, but increased susceptibility to PA14, a 'non-natural' pathogen
252 of the intestine.
253
254 **RNA-seq analysis of *pals-22/25*-upregulated genes define the IPR**
255 Previous work indicated that *N. parisii* and the Orsay virus induce a common set of
256 genes, despite these being very different pathogens [9]. We called eight of these genes
257 the IPR subset [6], and here we show they are regulated by *pals-22/25* (Fig 2A). To
258 identify additional genes regulated by *pals-22/25*, we performed RNA-seq analysis of
259 *pals-22* mutants, *pals-22 pals-25* mutants, and wild-type animals. We performed
260 differential gene expression analysis using a FDR<0.01 cutoff (see Materials and
261 Methods for a complete description of criteria) and determined that 2,756 genes were
262 upregulated in *pals-22* mutants compared to wild-type animals (Fig 5A, S7 Table). Next
263 we compared *pals-22* mutants to *pals-22 pals-25* double mutants and found that 744
264 genes were upregulated (Fig 5A, S7 Table). Of these two comparisons, there are 702
265 genes in common that are upregulated both in *pals-22* mutants compared to wild-type
266 animals and in *pals-22* mutants compared to *pals-22 pals-25* double mutants (Fig 5A).
267 Therefore, these 702 genes are negatively regulated by wild-type *pals-22* and require

268 the activity of the wild-type *pals-25* for their induction in the absence of *pals-22.* These
269 702 genes include genes like our *pals-5* reporter (Fig 1) and other IPR genes (Fig 2).
270
271 We next compared these 702 *pals-22/25* regulated genes to genes induced during *N.*
272 *parisii* infection identified in a previous study [9] to expand our list of IPR genes. Out of
273 127 genes induced during *N. parisii* infection we found that the *pals-22/25* gene pair
274 regulated mRNA expression of 80 of these genes (Fig 5A). Specifically, of the 25 *pals*
275 genes induced upon intracellular infection, all are induced in *pals-22* mutants and
276 reverted back to wild-type levels in *pals-22 pals-25* double mutants (Fig 5B, S7 Table).
277 Notably, all *pals* genes that are not regulated by *pals-22/25* are also not induced by
278 infection. Furthermore, the other nematode-specific genes F26F2.1, F26F2.3, and
279 F26F2.4, which are induced by *N. parisii* and Orsay virus infection, were also found to be
280 induced in *pals-22* mutants and brought back to wild-type levels in *pals-22 pals-25*
281 double mutants (Fig 5C). In addition, we found that the ubiquitin ligase components are
282 similarly regulated (Fig 5D). These studies thus define IPR genes as the 80 genes that
283 are: 1) induced by *N. parisii* infection, 2) induced in a *pals-22* mutant background, and 3)
284 reversed back to wild-type levels in *pals-22 pals-25* double mutants.
285
286 **Genes regulated by *pals-22/25* and infection are also regulated by proteasomal**
287 **stress**
288 Previous work indicated that blockade of the proteasome, either pharmacologically or
289 genetically, will induce expression of a subset of IPR genes [9]. To determine the IPR
290 genes that are induced by proteasome stress, we performed RNA-seq analysis to define
291 the whole-genome response to this stress. Again, we conducted differential expression
292 analysis and compared gene expression of animals after 4 hours of exposure to the

293 proteasome inhibitor bortezomib compared to the DMSO vehicle control. From these
294 experiments we determined that 988 genes are induced following bortezomib treatment,
295 using the cut-off mentioned above and described in the Materials and Methods.
296 Interestingly, nearly all of the IPR genes described above are also induced following
297 bortezomib treatment (Fig 5E). Previous work has shown that genes induced by *N.*
298 *parisii* do not include the proteasome subunits induced by proteasome blockade as part
299 of the bounceback response [9]. The bounceback response is induced via the
300 transcription factor SKN-1. Consistent with these results, here we find that the IPR genes
301 induced by bortezomib are distinct from those regulated by the transcription factor SKN-
302 1, as defined by a previous study [16]. The overlap between SKN-1 regulated genes and
303 IPR genes includes only one gene (Fig 5E).
304
305 As shown earlier, *pals-22* mutants have increased resistance to heat shock, and
306 previous work indicated that there is overlap between genes induced by chronic heat
307 stress and genes induced by *N. parisii* and virus infection [9]. However, the genes in
308 common are distinct from the canonical chaperones, or Heat Shock Proteins (HSPs),
309 which are induced by the heat shock transcription factor HSF-1. To learn more about the
310 connection between heat shock response, HSF-1, and the IPR, we compared the IPR
311 genes with those induced by HSF-1 as defined in a previous study [17]. Here we found 8
312 genes in common between our set of 80 IPR genes and the set of 368 genes
313 upregulated by HSF-1, none of which are predicted to encode chaperone proteins (S10
314 Table). We also compared the 368 genes upregulated by HSF-1 with the 702 genes that
315 are regulated by *pals-22/25* and found 59 genes in common (S10 Table). These genes
316 include secreted C-type lectins and F-box genes, but do not include chaperones. In

317 summary, HSF-1 regulates 59 genes in common with those regulated by *pals-22/25*, but
318 only 8 of these are IPR genes.
319
320 ***pals-22* and *pals-25* regulate expression of genes induced by other natural**
321 **pathogens**
322 Next, we used Gene Set Enrichment Analysis (GSEA) to broadly compare *pals-22/25*-
323 regulated genes to genes regulated by other pathogens, stressors, and stress-related
324 pathways. Here we found that *pals-22/25* does not significantly regulate expression of
325 genes induced by the Gram-negative bacterial pathogen *P. aeruginosa* or the Gram-
326 positive bacterial pathogens *Staphylococcus aureus* and *Enterococcus faecalis* as
327 analyzed in previous studies (Fig 6). Notably, the strains used in these studies are
328 clinical isolates. Furthermore, these pathogen species are not known to be natural
329 pathogens of nematodes and are not found inside *C. elegans* intestinal cells before there
330 is extensive tissue damage in the host [18]. (Refer to S9 Table for additional
331 comparisons among genes regulated by *pals-22/25*, bortezomib treatment, and other
332 pathogens and stress pathways.)
333
334 Because *pals-22* and *pals-25* regulate expression of a majority of the genes induced by
335 natural intestinal pathogens like *N. parisii* and the Orsay virus, we investigated whether
336 they regulate the transcriptional response to natural pathogens that infect other tissues.
337 The fungal pathogen *Drechmeria coniospora* infects and penetrates the epidermis of
338 nematodes, triggering a GPCR signaling pathway that upregulates expression of
339 neuropeptide-like (*nlp*) genes including *nlp-29* to promote defense [15]. Our
340 transcriptome analysis shows that *pals-22/25* regulate a significant number of genes in
341 common with *Drechmeria* infection (S10 Table). Notably these genes do not include the

342 well-characterized neuropeptide *nlp* defense genes, although they do include many of
343 the *pals* genes. A more recently described natural pathogen of *C. elegans* is
344 *Myzocytiopsis humicola,* which is an oomycete that also infects through the epidermis
345 and causes a lethal infection [19]. Here as well, *pals-22/25* regulate a significant number
346 of genes in common with those induced by *M. humicola* infection, including the chitinase-
347 like '*chil'* genes that promote defense against this pathogen (S10 Table). Interestingly,
348 these *chil* genes, like the *pals* genes, are species-specific [8, 19].
349
350 We next used Ortholist [20] to determine which genes identified from our RNA-seq
351 analyses have predicted human orthologs. Of the 702 genes regulated by *pals-22/25,*
352 279 genes (39.7%) have predicted human orthologs (S11 Table). In contrast, of the 368
353 genes induced in *hsf-1* mutants 190 (51.6%) have predicted human orthologs.
354 Therefore, more of the genes regulated by the conserved transcription factor *hsf-1* have
355 human orthologs compared to genes regulated by the *C. elegans*-specific *pals-22/25*
356 gene pair. Furthermore, when we restrict our analysis to just the 80 IPR genes, only 14
357 (17.5%) have predicted human orthologs, indicating that the transcriptional response to
358 natural infection is enriched for genes that are not well-conserved.
359
360 ***pals-22/25* control expression of epidermal defense genes induced by oomycetes**
361 As described above, the RNA-seq analysis of genes regulated by *pals-22/25* indicated
362 that this gene pair controls expression of genes induced by diverse natural pathogens of
363 *C. elegans*. Indeed, in a forward genetic screen for *C. elegans* genes that regulate
364 expression of the *M. humicola*-induced *chil-27p::GFP* reporter, we isolated independent
365 loss-of-function alleles of *pals-22* (Fig 7A). These mutant alleles cause constitutive
366 expression of *chil-27p::GFP* in the epidermis in the absence of infection (Fig 7B). RNAi

367 against *pals-22* also led to constitutive GFP expression (S12 Fig), in a manner that is
368 indistinguishable from that observed upon infection with *M. humicola*. These results
369 indicate that *pals-22* acts as a negative regulator of *chil-27* expression in the epidermis.
370
371 We then used a *pals-22; chil-27p::GFP* strain for a suppressor screen, analogous to the
372 one described earlier for suppressors of GFP expression in *pals-22; pals-5p::GFP* (Fig
373 1). Interestingly, in this new screen we isolated two new alleles of *pals-25* which fully
374 suppress the constitutive gene expression of *chil-27p::GFP* seen in *pals-22* mutants (Fig
375 7A-B), indicating that wild-type *pals-25* acts as a positive regulator of *chil-27* expression.
376 These observations are consistent with our differential expression analysis, which
377 determined that *chil-27* is induced in a *pals-22* mutant background and that *pals-25* is
378 required for this induction (Fig 7C). Therefore, *pals-22/25* act as a switch not only for
379 genes induced in the intestine by natural intestinal pathogens, but also as a switch for
380 genes induced in the epidermis by natural epidermal pathogens of *C. elegans*.
381
382 **Discussion**
383 In many organisms, there is a balance between growth and pathogen resistance. In
384 particular, many studies in plants have indicated that genetic immunity to disease comes
385 at a cost to the yield of crops [21]. Here we define a program in *C. elegans* that controls
386 a balance between organismal growth with resistance to natural pathogens, which is
387 regulated by the *pals-22/25* species-specific gene pair. These genes act as a switch
388 between a 'defense program' of enhanced resistance against diverse natural pathogens
389 like microsporidia and virus, improved tolerance of proteotoxic stress and increased
390 defense against exogenous RNA [8], and a 'growth program' of normal development and
391 lifespan (Fig 8). We call this physiological defense program the "IPR" and it appears to

392 be distinct from other canonical stress response pathways in *C. elegans*, including the
393 p38 MAP kinase pathway, the insulin-signaling pathway, and the heat shock response,
394 among others [6]. Our previous analyses indicated that ubiquitin ligases may play a role
395 in executing the IPR program, as the cullin/CUL-6 ubiquitin ligase subunit is required for
396 the enhanced proteostasis capacity of *pals-22* mutants [6].
397
398 *pals-22* mutants are highly resistant to the microsporidian pathogen *N. parisii*, which is
399 the most common parasite found in wild-caught *C. elegans* [22, 23]. Little is known about
400 innate immune pathways that provide defense against *N. parisii*. Canonical immune
401 pathways in *C. elegans* like the p38 MAP kinase pathway provide defense against most
402 pathogens tested in *C. elegans* but do not provide defense against *N. parisii* [12]. The
403 mechanism by which *pals-22/25* regulate resistance to *N. parisii* is not clear. Our RNA-
404 seq analysis demonstrates that *pals-22/25* affect expression of hundreds of genes in the
405 genome. In particular, most of the genes induced by the natural intracellular pathogens
406 Orsay virus and *N. parisii* are controlled by *pals-22* and *pals-25*, although the function of
407 these IPR genes in defense is unknown. Interestingly, we found that *pals-22/25* regulate
408 expression of genes induced not only by natural intestinal pathogens but also of genes
409 induced by natural epidermal pathogens, such as the oomycete species *M. humicola*. *M.*
410 *humicola* induces expression of *chil*-gene family, and genetic analysis shows these
411 genes promote defense against *M. humicola* [19]. Notably, we identified *pals-22/25* in
412 independent forward genetic screens for regulators of *chil-27* and found that they
413 regulate expression of this defense gene in the epidermis. Thus, *pals-22/25* regulate
414 expression of genes induced by diverse natural pathogens.
415

416 While *pals-25* is required to activate IPR gene expression in a *pals-22* mutant
417 background, it is not required for activation of IPR gene expression in response to *N.*
418 *parisii* infection or proteasomal stress. Therefore, *pals-22/25* may not mediate detection
419 of these pathogens, although they might mediate detection and be redundant with other
420 factors. Intriguingly, the *pals-22/25* gene pair share evolutionary and phenotypic features
421 with plant R gene pairs, which serve as sensors for virulence factors delivered into host
422 cells by co-evolved plant pathogens. For example, the *Arabidopsis thaliana* gene pair
423 RRS1 and RPS4 are species-specific, share the same promoter, and direct opposite
424 outcomes, with RRS1 inhibiting and RPS4 promoting 'effector-triggered immunity'
425 against natural pathogens [24, 25]. Similarly, *pals-22* and *pals-25* are species-specific,
426 appear to be in an operon together, and direct opposite physiological outcomes including
427 defense against natural pathogens. RRS1 and RPS4 proteins directly bind to each other,
428 and RRS1 normally inhibit RPS4 function until detection of bacterial virulence factors, at
429 which point RRS1 inhibition is relieved and RPS4 is free to promote pathogen defense,
430 although the steps downstream of RRS1/RPS4 are poorly understood. Although the *pals*
431 genes do not share sequence similarity with the R genes, in this analogy PALS-22 would
432 inhibit PALS-25 and serve as the 'tripwire' to detect virulence factors from natural
433 pathogens and free PALS-25 to promote the IPR defense program. While this model is
434 attractive, it is purely speculative as we currently have no direct evidence that PALS-22
435 detects virulence factors. Identification of such hypothetical virulence factors would be
436 the focus of future studies.
437
438 The molecular events by which *C. elegans* detects infection are poorly understood,
439 although nematodes do appear to use a form of effector-triggered immunity or
440 'surveillance immunity'. Studies with several distinct pathogens have indicated that *C.*

441 *elegans* induces defense gene expression in response to perturbation of core processes
442 like translation and the ubiquitin-proteasome system [26]. For example, studies with *P.*
443 *aeruginosa* demonstrated that *C. elegans* detects the presence of the translation-
444 blocking Exotoxin A through its effects on host translation, not through detection of the
445 shape of the toxin [27, 28]. In addition to this mode of detection, *C. elegans* may also
446 detect specific molecular signatures like canonical Pathogen-Associated Molecular
447 Patterns (PAMPs). In all likelihood, several types of pathogen detection are used by *C.*
448 *elegans*. Surprisingly however, there have been no direct PAMP ligand/receptor
449 interactions demonstrated for pattern recognition receptors (PRR) in the worm, although
450 there has been a Damage-Associated Molecular Pattern (DAMP)/G-protein-coupled
451 receptor interaction demonstrated to be critical for response to *Drechmeria* infection [29].
452 Indeed, *C. elegans* lacks many PRR signaling pathways that are well described in flies
453 and mammals. For example, the *C. elegans* single Toll-like receptor *tol-1* does not act
454 canonically and worms appear to have lost its downstream transcription factor NFkB,
455 which is critical for innate immunity in flies and mammals [30]. Perhaps conservation of
456 immune genes is only reserved for defense against rare, 'non-natural' pathogens,
457 because genes that are important for immunity are subject to attack and inhibition by
458 microbes [31]. Thus, immune genes that provide defense against natural pathogens from
459 the recent evolutionary past will not be broadly conserved but rather will be species-
460 specific, like rapidly evolving R genes in plants. While R genes have been shown to
461 encode proteins that detect virulence factors secreted into host cells by co-evolved plant
462 pathogens, the mechanism by which they activate downstream immune signaling is
463 unclear. We propose that the IPR physiological program regulated by the *pals-22/25*
464 antagonistic paralogs in *C. elegans* could be analogous to effector-triggered immunity

465 regulated by opposing R gene pairs like RRS1/RPS4 used in plants for resistance
466 against co-evolved pathogens.
467
468 Interestingly, an example of vertebrate-specific antagonistic paralogs has recently been
469 described to play a role in regulating nonsense-mediated RNA decay (NMD) [32]. These
470 studies provide a potential explanation to the long-standing question of how gene
471 duplications are retained, when they are presumably redundant immediately following
472 gene duplication. Specifically, this model predicts that gene duplication events can be
473 rapidly retained if the proteins made from these genes are involved in protein-protein
474 interactions. With just one non-synonymous nucleotide change that switches a wild-type
475 copy to become dominant negative within a multimeric signaling complex, a gene
476 duplication event can be selected for and retained in the heterozygote state – i.e. in one
477 generation. Perhaps in this way, new genes can be born and survive, when gene pairs
478 can evolve to direct opposing functions like the Upf3a/3b paralogs in NMD, and the
479 RRS1/RPS4 and *pals-22/25* paralogs in immunity/growth.
480
481
482
483 **Methods**
484 *Strains*
485 *C. elegans* were maintained at 20°C on Nematode Growth Media (NGM) plates seeded
486 with Streptomycin-resistant *E. coli* OP50-1 bacteria according to standard methods [33].
487 We used N2 wild-type animals. Mutant or transgenic strains were backcrossed at least
488 three times. See S1 Table for a list of all strains used in this study.
489

490 *EMS screens and cloning of alleles*

491 *pals-22* mutant worms (either the *jy1* or *jy3* allele) carrying the *jyIs8[pals-5p::GFP, myo-*
492 *2p::mCherry]* transgene were mutagenized with ethyl methane sulfonate (EMS) (Sigma)
493 using standard procedures as described [34]. L4 stage P0 worms were incubated in 47
494 mM EMS for 4 hours at 20°C. Worms were screened in the F2 generation for decreased
495 expression of GFP using the COPAS Biosort machine (Union Biometrica).
496 Complementation tests were carried out by generating worms heterozygous for two
497 mutant alleles and scoring *pals-5p::GFP* fluorescence. For whole-genome sequencing
498 analysis of mutants, genomic DNA was prepared using a Puregene Core kit (Qiagen)
499 and 20X sequencing coverage was obtained. We identified only one gene (*pals-25*) on
500 LGIII containing variants predicted to alter function in both mutants sequenced (*jy9* and
501 *jy100*). Additional *pals-25* alleles were identified by Sanger sequencing. Screens in the
502 strains carrying the *icbIs4[chil-27p::GFP, col-12p::mCherry]* transgene were performed
503 in a similar manner except that we used 24 mM EMS to recover the *pals-22* alleles
504 (*icb88*, *icb90*) and 17 mM EMS for the *pals-22(icb90)* suppressor screen and that in both
505 cases we selected F2 animals manually using a Zeiss Axio ZoomV16 dissecting scope.
506 The two *pals-22* alleles (*icb88*, *icb90*) were identified by whole genome sequencing of
507 GFP positive F2 recombinants after crossing to the polymorphic isolate CB4856 as
508 previously described [35] whereas the two *pals-25* alleles were found by direct
509 sequencing of the mutant strains. The *pals-22(icb89)* allele was identified by Sanger
510 sequencing. See S1 Table for a list of all mutations identified.

511

512 *RNA interference*

513 RNA interference was performed using the feeding method. Overnight cultures of RNAi
514 clones in the HT115 bacterial strain were seeded onto NGM plates supplemented with

515 5mM IPTG and 1mM carbenicillin and incubated at 25°C for 1 day. Eggs from bleached
516 parents or synchronized L1 stage animals were fed RNAi until the L4 stage at 20°C. For
517 all RNAi experiments an *unc-22* clone leading to twitching animals was used as a
518 positive control to test the efficacy of the RNAi plates. The *pals-22* RNAi clone (from the
519 Ahringer RNAi library) was verified by sequencing. The *pals-25* RNAi clone was made
520 with PCR and includes 1079 base pairs spanning the second, third, and fourth exons of
521 *pals-25*. This sequence was amplified from N2 genomic DNA, cloned into the L4440
522 RNAi vector, and then transformed into HT115 bacteria for feeding RNAi experiments.

523 *Quantitative RT-PCR*

524 Endogenous mRNA expression changes were measured with qRT-PCR as previously
525 described [6]. Synchronized L1 worms were grown on NGM plates at 20°C to the L4
526 stage and then collected in TriReagent (Molecular Research Center, Inc.) for RNA
527 extraction. For *N. parisii* infection, 7 x 10^6 spores were added to plates with L4 stage
528 worms and then incubated at 25°C for 4 hours before RNA isolation. Bortezomib (or an
529 equivalent amount of DMSO) was added to L4 stage worms for a final concentration of
530 20 µM; plates were then incubated at 20°C for 4 hours before RNA isolation. At least two
531 independent biological replicates were measured for each condition, and each biological
532 replicate was measured in duplicate and normalized to the *snb-1* control gene, which did
533 not change upon conditions tested. The Pffafl method was used for quantifying data [36].

534 *Heat shock assay*

535 Worms were grown on standard NGM plates until the L4 stage at 20°C and then shifted
536 to 37°C for two hours. Following heat shock, plates were laid in a single layer on the
537 bench top for 30 minutes to recover, and then moved to a 20°C incubator overnight.
538 Worms were scored in a blinded manner for survival 24 hours after heat shock; animals

539 not pumping or responding to touch were scored as dead. Three plates were assayed for
540 each strain in each replicate, with at least 30 worms per plate, and three independent
541 assays were performed.
542
543 *GFP fluorescence measurement*
544 Synchronized L1 stage animals were grown at 20°C to the L4 stage. The COPAS Biosort
545 machine (Union Biometrica) was used to measure the time of flight (as a measure of
546 length) and fluorescence of individual worms. At least 100 worms were measured for
547 each strain, and all experiments were repeated three times.
548
549 *Lifespan*
550 L4 stage worms were transferred to 6 cm NGM plates seeded with OP50-1 bacteria and
551 incubated at 25°C. Worms were scored every day, and animals that did not respond to
552 touch were scored as dead. Animals that died from internal hatching or crawled off the
553 plate were censored. Worms were transferred to new plates every day throughout the
554 reproductive period. Three plates were assayed for each strain in each replicate, with 40
555 worms per plate.
556
557 *Microscopy*
558 Worms were anesthetized with 10 µM levamisole in M9 buffer and mounted on 2%
559 agarose pads for imaging. Images in Figure S1B and S1C were captured with a Zeiss
560 LSM700 confocal microscope. All other *C. elegans* images were captured with a Zeiss
561 AxioImager M1 or Axio Zoom.V16.
562
563 *N. parisii and Orsay virus infection assays*

564 *N. parisii* spores were prepared as previously described [37], and Orsay virions were
565 prepared as described previously [9]. For pathogen load analysis, synchronized L1
566 worms were plated with a mixture of OP50 bacteria and 5 x 10^5 *N. parisii* spores or a
567 1:20 dilution of Orsay virus filtrate, and then incubated at 25°C for either 30 hours (*N.*
568 *parisii*) or 18 hours (Orsay virus) before fixing with paraformaldehyde. Fixed worms were
569 stained with individual FISH probes conjugated to the red Cal Fluor 610 dye (Biosearch
570 Technologies) targeting either *N. parisii* ribosomal RNA or Orsay virus RNA. *N. parisii*
571 pathogen load was measured with the COPAS Biosort machine (Union Biometrica).
572 Orsay virus infection was assayed visually using the 10x objective on a Zeiss
573 AxioImager M1 microscope. In feeding measurement assays, plates were set up as for
574 pathogen infection with the addition of fluorescent beads (Fluoresbrite Polychromatic
575 Red Microspheres, Polysciences Inc.). Worms were fixed in paraformaldehyde after 30
576 minutes and red fluorescence signal was measured with the COPAS Biosort machine
577 (Union Biometrica).
578
579 *P. aeruginosa pathogen load*
580 Overnight cultures of a *P. aeruginosa* PA14-dsRed strain [38] were seeded onto SK
581 plates with 50 µg/ml ampicillin, and then incubated at 37°C for 24 hours followed by
582 25°C for 24 hours. Worms at the L4 stage were washed onto the PA14-dsRed plates,
583 incubated at 25°C for 16 hours, and then assayed with a COPAS Biosort machine
584 (Union Biometrica) for the amount of red fluorescence inside each animal.
585
586 *RNA-seq sample preparation*
587 Synchronized L1 stage worms were grown on 10 cm NGM plates seeded with OP50-1
588 *E. coli* at 20°C until worms had reached the L4 stage. N2, *pals-22(jy3)*, and *pals-22(jy3)*

589 *pals-25(jy9)* strains were then shifted to 25°C for 4 hours before harvesting for RNA
590 extraction. Bortezomib (or an equivalent amount of DMSO) was added to plates with L4
591 stage N2 worms for a final concentation of 20uM; plates were then incubated at 20°C for
592 4 hours before RNA isolation. RNA was isolated with TriReagent purification, followed by
593 RNeasy column cleanup (Qiagen), as described [39]. RNA quality was assessed by
594 Tapestation analysis at the Institute for Genomic Medicine (IGM) at UC San Diego.
595 Paired-end sequencing libraries were then constructed with the TruSeq Stranded mRNA
596 method (Illumina), followed by sequencing on HiSeq4000 machine (Illumina).
597
598 *RNA-seq analysis*
599
600 Sequencing reads were aligned to WormBase release WS235 using Bowtie 2 [40], and
601 transcript abundance was estimated using RSEM [41]. Differential expression analysis
602 was performed in RStudio (v1.1.453) [42] using R (v3.50) [43] and Bioconductor (v3.7)
603 [44] packages. As outlined in the RNAseq123 vignette [45], data was imported, filtered
604 and normalized using edgeR [46], and linear modeling and differential expression
605 analysis was performed using limma [47]. An FDR [48] cutoff of <0.01 was used to
606 define differentially expressed genes; no fold-change criteria was used. Lists of
607 upregulated genes used for comparisons were exported and further sanitized to remove
608 dead genes and update WBGeneIDs to Wormbase release WS263.
609
610 *Functional analysis*
611 Functional analysis was performed using Gene Set Enrichment Analysis (GSEA) v3.0
612 software [49, 50]. Normalized RNA-seq expression data were converted into a GSEA-
613 compatible filetype and ranked using the signal-to-noise metric with 1,000 permutations.
614 Gene sets from other studies were converted to WBGeneIDs according to WormBase

release WS263. Independent analyses were performed for each of three comparisons: untreated *pals-22(jy3)* versus untreated N2 animals; untreated *pals-22(jy3)* versus untreated *pals-22(jy3) pals-25(jy9)* animals; bortezomib treated N2 versus DMSO vehicle control treated N2. Results were graphed based on their NES-value using GraphPad Prism 7 (GraphPad Software, La Jolla, CA).

Acknowledgments

We acknowledge the IGM for RNAseq library construction and sequencing, Corrina Elder, Jessica Sowa, Ivana Sfarcic, and Michael K. Fasseas for technical support, and Vladimir Lazetic, Robert Luallen, Johan Panek, Ivana Sfarcic, Eillen Tecle, Samira Yitiz and Elina Zuniga for comments on the manuscript.

References

1. Pearson JC, Lemons D, McGinnis W. Modulating Hox gene functions during animal body patterning. Nature Reviews Genetics. 2005;6(12):893.
2. Ross BD, Rosin L, Thomae AW, Hiatt MA, Vermaak D, de la Cruz AFA, et al. Stepwise evolution of essential centromere function in a Drosophila neogene. Science. 2013;340(6137):1211-4.
3. Joshi RK, Nayak S. Perspectives of genomic diversification and molecular recombination towards R-gene evolution in plants. Physiology and Molecular Biology of Plants. 2013;19(1):1-9.
4. von Moltke J, Ayres JS, Kofoed EM, Chavarría-Smith J, Vance RE. Recognition of bacteria by inflammasomes. Annual review of immunology. 2013;31:73-106.
5. Li X, Kapos P, Zhang Y. NLRs in plants. Current opinion in immunology. 2015;32:114-21.

644 6. Reddy KC, Dror T, Sowa JN, Panek J, Chen K, Lim ES, et al. An intracellular
645 pathogen response pathway promotes proteostasis in C. elegans. Current Biology.
646 2017;27(22):3544-53. e5.
647 7. Hentati A, Bejaoui K, Pericak-Vance MA, Hentati F, Speer MC, Hung W-Y, et al.
648 Linkage of recessive familial amyotrophic lateral sclerosis to chromosome 2q33–
649 q35. Nature genetics. 1994;7(3):425.
650 8. Leyva-Díaz E, Stefanakis N, Carrera I, Glenwinkel L, Wang G, Driscoll M, et al.
651 Silencing of repetitive DNA is controlled by a member of an unusual Caenorhabditis
652 elegans gene family. Genetics. 2017;207(2):529-45.
653 9. Bakowski MA, Desjardins CA, Smelkinson MG, Dunbar TA, Lopez-Moyado IF,
654 Rifkin SA, et al. Ubiquitin-mediated response to microsporidia and virus infection in
655 C. elegans. PLoS pathogens. 2014;10(6):e1004200.
656 10. Zuryn S, Jarriault S, editors. Deep sequencing strategies for mapping and
657 identifying mutations from genetic screens. Worm; 2013: Taylor & Francis.
658 11. Sarov M, Murray JI, Schanze K, Pozniakovski A, Niu W, Angermann K, et al. A
659 genome-scale resource for in vivo tag-based protein function exploration in C.
660 elegans. Cell. 2012;150(4):855-66.
661 12. Troemel ER, Félix M-A, Whiteman NK, Barrière A, Ausubel FM. Microsporidia
662 are natural intracellular parasites of the nematode Caenorhabditis elegans. PLoS
663 biology. 2008;6(12):e309.
664 13. Raizen DM, Lee R, Avery L. Interacting genes required for pharyngeal
665 excitation by motor neuron MC in Caenorhabditis elegans. Genetics.
666 1995;141(4):1365-82.
667 14. Félix M-A, Ashe A, Piffaretti J, Wu G, Nuez I, Bélicard T, et al. Natural and
668 experimental infection of Caenorhabditis nematodes by novel viruses related to
669 nodaviruses. PLoS biology. 2011;9(1):e1000586.
670 15. Kim D, Ewbank J. Signaling in the Immune Response. 2015 Dec 22.
671 WormBook [Internet] http://wwwwormbookorg.1-51.
672 16. Oliveira RP, Abate JP, Dilks K, Landis J, Ashraf J, Murphy CT, et al. Condition -
673 adapted stress and longevity gene regulation by Caenorhabditis elegans SKN -
674 1/Nrf. Aging cell. 2009;8(5):524-41.
675 17. Li J, Chauve L, Phelps G, Brielmann RM, Morimoto RI. E2F coregulates an
676 essential HSF developmental program that is distinct from the heat-shock response.
677 Genes Dev. 2016;30(18):2062-75. Epub 2016/11/01. doi: 10.1101/gad.283317.116.
678 PubMed PMID: 27688402; PubMed Central PMCID: PMCPMC5066613.
679 18. Irazoqui JE, Troemel ER, Feinbaum RL, Luhachack LG, Cezairliyan BO,
680 Ausubel FM. Distinct pathogenesis and host responses during infection of C. elegans
681 by P. aeruginosa and S. aureus. PLoS pathogens. 2010;6(7):e1000982.
682 19. Osman GA, Fasseas MK, Koneru SL, Essmann CL, Kyrou K, Srinivasan MA, et
683 al. Natural infection of C. elegans by an oomycete reveals a new pathogen-specific
684 immune response. Current Biology. 2018;28(4):640-8. e5.
685 20. Shaye DD, Greenwald I. OrthoList: a compendium of C. elegans genes with
686 human orthologs. PloS one. 2011;6(5):e20085.
687 21. Ning Y, Liu W, Wang G-L. Balancing Immunity and Yield in Crop Plants.
688 Trends in plant science. 2017.

689 22. Schulenburg H, Félix M-A. The natural biotic environment of Caenorhabditis
690 elegans. Genetics. 2017;206(1):55-86.
691 23. Zhang G, Sachse M, Prevost M-C, Luallen RJ, Troemel ER, Félix M-A. A large
692 collection of novel nematode-infecting microsporidia and their diverse interactions
693 with Caenorhabditis elegans and other related nematodes. PLoS pathogens.
694 2016;12(12):e1006093.
695 24. Le Roux C, Huet G, Jauneau A, Camborde L, Trémousaygue D, Kraut A, et al. A
696 receptor pair with an integrated decoy converts pathogen disabling of transcription
697 factors to immunity. Cell. 2015;161(5):1074-88.
698 25. Sarris PF, Duxbury Z, Huh SU, Ma Y, Segonzac C, Sklenar J, et al. A plant
699 immune receptor detects pathogen effectors that target WRKY transcription factors.
700 Cell. 2015;161(5):1089-100.
701 26. Cohen LB, Troemel ER. Microbial pathogenesis and host defense in the
702 nematode C. elegans. Current opinion in microbiology. 2015;23:94-101.
703 27. Dunbar TL, Yan Z, Balla KM, Smelkinson MG, Troemel ER. C. elegans detects
704 pathogen-induced translational inhibition to activate immune signaling. Cell host &
705 microbe. 2012;11(4):375-86.
706 28. McEwan DL, Kirienko NV, Ausubel FM. Host translational inhibition by
707 Pseudomonas aeruginosa Exotoxin A Triggers an immune response in
708 Caenorhabditis elegans. Cell host & microbe. 2012;11(4):364-74.
709 29. Zugasti O, Bose N, Squiban B, Belougne J, Kurz CL, Schroeder FC, et al.
710 Activation of a G protein-coupled receptor by its endogenous ligand triggers the
711 Caenorhabditis elegans innate immune response. Nature immunology.
712 2014;15(9):833.
713 30. Irazoqui JE, Urbach JM, Ausubel FM. Evolution of host innate defence:
714 insights from Caenorhabditis elegans and primitive invertebrates. Nature Reviews
715 Immunology. 2010;10(1):47.
716 31. Maltez VI, Miao EA. Reassessing the evolutionary importance of
717 inflammasomes. The Journal of Immunology. 2016;196(3):956-62.
718 32. Shum EY, Jones SH, Shao A, Dumdie J, Krause MD, Chan W-K, et al. The
719 antagonistic gene paralogs Upf3a and Upf3b govern nonsense-mediated RNA decay.
720 Cell. 2016;165(2):382-95.
721 33. Brenner S. The genetics of Caenorhabditis elegans. Genetics. 1974;77(1):71-
722 94.
723 34. Kutscher LM, Shaham S. Forward and reverse mutagenesis in C. elegans.
724 WormBook: the online review of C elegans biology. 2014:1.
725 35. Minevich G, Park DS, Blankenberg D, Poole RJ, Hobert O. CloudMap: a cloud-
726 based pipeline for analysis of mutant genome sequences. Genetics.
727 2012;192(4):1249-69.
728 36. Pfaffl MW. A new mathematical model for relative quantification in real-time
729 RT–PCR. Nucleic acids research. 2001;29(9):e45-e.
730 37. Balla KM, Andersen EC, Kruglyak L, Troemel ER. A wild C. elegans strain has
731 enhanced epithelial immunity to a natural microsporidian parasite. PLoS pathogens.
732 2015;11(2):e1004583.

733 38. Djonović S, Urbach JM, Drenkard E, Bush J, Feinbaum R, Ausubel JL, et al.
734 Trehalose biosynthesis promotes Pseudomonas aeruginosa pathogenicity in plants.
735 PLoS pathogens. 2013;9(3):e1003217.
736 39. Troemel ER, Chu SW, Reinke V, Lee SS, Ausubel FM, Kim DH. p38 MAPK
737 regulates expression of immune response genes and contributes to longevity in C.
738 elegans. PLoS genetics. 2006;2(11):e183.
739 40. Langmead B, Salzberg SL. Fast gapped-read alignment with Bowtie 2. Nature
740 methods. 2012;9(4):357.
741 41. Li B, Dewey CN. RSEM: accurate transcript quantification from RNA-Seq data
742 with or without a reference genome. BMC bioinformatics. 2011;12(1):323.
743 42. Team R. RStudio: integrated development for R. RStudio, Inc, Boston, MA URL
744 http://wwwrstudiocom. 2015.
745 43. Team RC. R: A language and environment for statistical computing. 2013.
746 44. Gentleman RC, Carey VJ, Bates DM, Bolstad B, Dettling M, Dudoit S, et al.
747 Bioconductor: open software development for computational biology and
748 bioinformatics. Genome biology. 2004;5(10):R80.
749 45. Law CW, Alhamdoosh M, Su S, Smyth GK, Ritchie ME. RNA-seq analysis is
750 easy as 1-2-3 with limma, Glimma and edgeR. F1000Research. 2016;5.
751 46. Robinson MD, McCarthy DJ, Smyth GK. edgeR: a Bioconductor package for
752 differential expression analysis of digital gene expression data. Bioinformatics.
753 2010;26(1):139-40.
754 47. Ritchie ME, Phipson B, Wu D, Hu Y, Law CW, Shi W, et al. limma powers
755 differential expression analyses for RNA-sequencing and microarray studies.
756 Nucleic acids research. 2015;43(7):e47-e.
757 48. Storey JD, Tibshirani R. Statistical significance for genomewide studies.
758 Proceedings of the National Academy of Sciences. 2003;100(16):9440-5.
759 49. Mootha VK, Lindgren CM, Eriksson K-F, Subramanian A, Sihag S, Lehar J, et al.
760 PGC-1α-responsive genes involved in oxidative phosphorylation are coordinately
761 downregulated in human diabetes. Nature genetics. 2003;34(3):267.
762 50. Subramanian A, Tamayo P, Mootha VK, Mukherjee S, Ebert BL, Gillette MA, et
763 al. Gene set enrichment analysis: a knowledge-based approach for interpreting
764 genome-wide expression profiles. Proceedings of the National Academy of Sciences.
765 2005;102(43):15545-50.
766

767

768

769 **Figure Legends**

770

771 **Fig 1. *pals-25* is required for increased *pals-5p::GFP* expression in *pals-22***

772 **mutants.**

773 (A-E) Mutants isolated from *pals-22* suppressor screens show decreased expression of

774 the *pals-5p::GFP* reporter. Shown are (A) wild-type, (B) *pals-22(jy1)*, (C) *pals-22(jy3)*, (D)

775 *pals-22(jy1) pals-25(jy11)*, and (E) *pals-22(jy3) pals-25(jy9)* animals. Green is *pals-*

776 *5p::GFP*, red is *myo-2p::mCherry* expression in the pharynx as a marker for presence of

777 the transgene. Images are overlays of green, red and Nomarski channels and were

778 taken with the same camera exposure for all. Scale bar, 100 μm. (F) *pals-5p::GFP*

779 expression quantified in *pals-22* suppressor mutants using a COPAS Biosort machine to

780 measure the mean GFP signal and length of individual animals, indicated by green dots.

781 Mean signal of the population is indicated by black bars, with error bars as SD. Graph is

782 a compilation of three independent replicates, with at least 100 animals analyzed in each

783 replicate. *** $p < 0.001$ with Student's t-test. (G) *pals-22* and *pals-25* gene coding

784 structure (UTR not shown), with blue exons for *pals-22* and red exons for *pals-25*. See

785 S1 Table for residues altered. (H) *pals-5p::GFP* expression in animals treated with either

786 L4440 RNAi control or *pals-25* RNAi, quantified using a COPAS Biosort machine to

787 measure the mean GFP signal and length of animals. Parameters the same as in (F).

788

789

790 **Fig 2. *pals-25* is required for increased IPR gene expression in *pals-22* mutants,**

791 **but not for IPR induction in response to infection or proteasome inhibition.**

792 (A) qRT-PCR measurement of gene expression in *pals-22* and *pals-22 pals-25* animals,

793 shown as the fold change relative to wild-type control. (B-C) qRT-PCR measurement of

794 IPR gene expression in *pals-22(jy3)* and *pals-22(jy3) pals-25(jy9)* animals following 4
795 hours of infection with *N. parisii* (B) or treatment with the proteasome inhibitor
796 bortezomib (C). For (A-C), results shown are the average of two independent biological
797 replicates and error bars are SD. * $p < 0.05$ with Student's t-test.
798
799
800 **Fig 3. *pals-25* mutations suppress diverse phenotypes of *pals-22* mutants.**
801 (A) *pals-25* mutation suppresses the developmental delay of *pals-22* mutants. Fraction of
802 animals reaching the L4 larval stage 48 hours after eggs were laid is indicated. Results
803 shown are the average of three independent biological replicates, with 100 animals
804 assayed in each replicate. Error bars are SD. *** $p < 0.001$ with Student's t-test. (B)
805 Lifespan of wild type, *pals-22(jy3)*, and *pals-22(jy3) pals-25(jy9)* animals. Assays were
806 performed with 40 animals per plate, and three plates per strain per experiment. This
807 experiment was repeated three independent times with similar results, with data from a
808 representative experiment shown. See Figures S2A and S2B for other replicates. p-value
809 for *pals-22(jy3)* compared to *pals-22(jy3) pals-25(jy9)* is <0.0001 using the Log-rank test.
810 (C) The increased survival of *pals-22* mutants after heat shock is suppressed by
811 mutations of *pals-25*. Animals were incubated for 2 hours at 37°C followed by 24 hours
812 at 20°C, and then assessed for survival. Strains were tested in triplicate, with at least 30
813 animals per plate. Mean fraction alive indicates the average survival among the
814 triplicates, errors bars are SD. ** $p < 0.01$. Assay was repeated three independent times
815 with similar results, and data from a representative experiment are shown. See Figures
816 S2C and S2D for other replicates. (D-I) *pals-25* mutation suppresses transgene silencing
817 in *pals-22* mutants. (D) *ric-19p::GFP* expression quantified in *pals-22* and *pals-22 pals-*
818 *25* mutants using a COPAS Biosort machine to measure the mean GFP signal and

819 length of individual animals, indicated by green dots. Mean signal of the population is
820 indicated by black bars with error bars as SD. Graph is a compilation of three
821 independent replicates, with at least 100 animals analyzed in each replicate. *** $p <$
822 0.001 with Student's t-test. In (E-I), green is neuronal expression of *ric-19p::GFP*. Shown
823 are (E) wild-type, (F) *pals-22(jy1)*, (G) *pals-22(jy3)*, (H) *pals-22(jy1) pals-25(jy11)*, and (I)
824 *pals-22(jy3) pals-25(jy9)* animals. Images are overlays of green and Nomarski channels
825 and were taken with the same camera exposure for all. Scale bar, 100 μm.
826
827
828 **Figure 4. *pals-22* mutants have increased resistance to infection by *N. parisii* or**
829 **Orsay virus, dependent on *pals-25*.**
830 (A-E) Images of (A) wild-type, (B) *pals-22(jy1)*, (C) *pals-22(jy3)*, (D) *pals-22(jy1) pals-*
831 *25(jy11)*, and (E) *pals-22(jy3) pals-25(jy9)* animals infected with *N. parisii* as L1s, fixed
832 30 hours post infection, and stained by FISH with an *N. parisii*-specific probe (red). Scale
833 bar, 100 μm. (F) *N. parisii* FISH signal quantified using a COPAS Biosort machine to
834 measure the mean red signal and length of individual animals, indicated by red dots.
835 Mean signal of the population is indicated by black bars, with error bars as SD. Graph is
836 a compilation of three independent replicates, with at least 100 animals analyzed in each
837 replicate. *** $p < 0.001$ with Student's t-test. (G) Fraction of animals infected with the
838 Orsay virus 18 hours post infection is indicated. Animals were fixed and stained by FISH
839 with a virus-specific probe, and scored visually for infection. Results shown are the
840 average of three independent biological replicates, with 100 animals assayed in each
841 replicate. Error bars are SD. *** $p < 0.001$ with Student's t-test. (H-L) Images of (H) wild-
842 type, (I) *pals-22(jy1)*, (J) *pals-22(jy3)*, (K) *pals-22(jy1) pals-25(jy11)*, and (L) *pals-22(jy3)*
843 *pals-25(jy9)* animals infected with the Orsay virus as L1s, fixed 18 hours post infection,

844 and stained by FISH with a virus-specific probe (red). Scale bar, 100 μm. (M)
845 Quantification of dsRed fluorescence levels in wild-type, *pals-22*, and *pals-22 pals-25*
846 animals after 16 hours of exposure to dsRed-expressing PA14. Red fluorescence was
847 measured using a COPAS Biosort machine to measure the mean red signal and length
848 of individual animals, indicated by red dots. Mean signal of the population is indicated by
849 black bars, with error bars as SD. Graph is a compilation of three replicates, with at least
850 100 animals analyzed in each replicate. *** $p < 0.001$ with Student's t-test.
851
852
853 **Fig 5. The *pals-22/25* gene pair transcriptionally regulates genes that are induced**
854 **by *N. parisii* infection or proteasome blockade**
855 (A) Venn diagram comparing 1) genes upregulated in *pals-22* mutants compared to wild-
856 type animals, 2) genes upregulated in *pals-22* mutants compared to *pals-22 pals-25*
857 double mutants and 3) genes induced in wild-type animals in response to *N. parisii*
858 infection. Gene sets 1 and 2 were obtained from RNA-seq data outlined in this study,
859 and Gene set 3 was obtained via RNA-seq in a previous study [9]. We define the IPR
860 genes as the 80 genes common across the three gene sets. (B-D) The relative mRNA
861 levels measured by RNA-seq in: *pals-22(jy3)* animals compared to wild-type; *pals-*
862 *22(jy3) pals-25(jy9)* animals compared to wild-type; and wild-type animals treated with
863 the proteasome inhibitor bortezomib (BTZ) compared to DMSO (vehicle control for BTZ).
864 * FDR<0.01 as calculated by edgeR and limma (see Materials and Methods) indicates
865 the gene is considered to be differentially expressed. (B) *pals* genes induced by *N.*
866 *parisii* infection are also regulated by *pals-22/25* and induced by BTZ. (C) Species-
867 specific F26F2 genes are regulated by the *pals-22/25* gene pair and are induced by BTZ.
868 (D) The Cullin-Ring Ligase components Cullin (*cul)* and Skp-related (*skr)* genes that are

869 upregulated during *N. parisii* infection are also regulated by the *pals-22/25* gene pair and
870 induced by BTZ. (E) Venn Diagram showing overlap between: IPR genes defined in (A);
871 genes upregulated by treatment with BTZ; and genes upregulated due to *skn-1* RNAi
872 [16]. See Tables S2 and S3 for detailed expression levels of genes discussed here.
873
874
875 **Fig 6. Functional analysis of genes transcriptionally regulated by the *pals-22/25***
876 **gene pair**
877 Correlation of genes transcriptionally regulated by the *pals-22/25* gene pair and genes
878 differentially expressed due to bortezomib treatment with genes that are up- or
879 downregulated in response to infection by pathogens or other environmental stresses.
880 Analysis was performed using the GSEA 3.0 software package (see Materials and
881 Methods) and correlation is quantified as a Normalized Enrichment Score (NES). A
882 positive NES (yellow) indicates correlation with upregulated genes in the denoted
883 comparison while a negative NES (blue) indicates correlation with downregulated genes.
884 Black cells indicate no significant correlation was detected, a FDR>0.25, or p>0.05).
885 *FDR<0.05. For more detailed results, see S9 Table. For details on the gene sets used
886 see S8 Table.
887
888 **Fig 7. *pals-22* and *pals-25* regulate expression of *chil-27* in the epidermis.**
889 (A) *pals-22* and *pals-25* gene coding structure (UTR not shown), with blue exons for
890 *pals-22* and red exons for *pals-25*. See S1 Table for residues altered. (B) Expression of
891 *chil-27p::GFP* is regulated by *pals-22* and *pals-25*. Shown are control, *pals-22(icb88)*,
892 *pals-22(icb90)*, *pals-22(icb90) pals-25(icb91)*, and *pals-22(icb90) pals-25(icb92)*
893 animals. The *col-12p::mCherrry* transgene is constitutively expressed in the epidermis.

894 Scale bar, 100 μm. (C) Relative levels of *chil* gene expression. *pals-22/25* regulate *chil*
895 genes that are induced upon infection by oomycete. *FDR<0.01 as calculated by edgeR
896 and limma (see Materials and Methods) indicates the gene is considered to be
897 differentially expressed.
898
899 **Fig 8. Model for *pals-22/pals-25* regulation of response to natural pathogens of *C.***
900 ***elegans*.**
901
902
903 **Supporting information**
904
905 **S1 Table. Lists of strains and mutations.**
906
907 **S2 Figure. *pals-25* RNAi suppresses increased *pals-5p::GFP* expression in *pals-22***
908 **mutants and PALS-25::GFP is expressed broadly.**
909 (A) Wild-type or *pals-22* mutant animals carrying the *pals-5p::GFP* transgene, treated
910 with either L4440 RNAi control or *pals-25* RNAi. Green is *pals-5p::GFP*, red is *myo-*
911 *2p::mCherry* expression in the pharynx as a marker for presence of the transgene.
912 Images are overlays of green, red, and Nomarski channels and were taken with the
913 same camera exposure for all. Scale bar, 100 μm. (B,C) Confocal fluorescence images
914 of adult animals carrying a fosmid transgene expressing PALS-25::GFP from the
915 endogenous promoter. Animals were treated with either (B) L4440 RNAi control or (C)
916 *pals-22* RNAi. Scale bar, 50 μm.
917

918 **S3 Figure. *pals-25* mutation suppresses the lifespan and thermotolerance**
919 **phenotypes of *pals-22* mutants.**
920 (A,B) Lifespan of wild type, *pals-22(jy3)*, and *pals-22(jy3) pals-25(jy9)* animals. Assays
921 were performed with 40 animals per plate, and three plates per strain per experiment. p-
922 value for *pals-22(jy3)* compared to *pals-22(jy3) pals-25(jy9)* is <0.0001 using the Log-
923 rank test. (C,D) Survival of animals after 2 hour heat shock treatment at 37°C followed
924 by 24 hours at 20°C. Strains were tested in triplicate, with at least 30 animals per plate.
925 Mean fraction alive indicates the average survival among the triplicates, errors bars are
926 SD. ** $p < 0.01$, * $p < 0.05$.
927
928 **S4 Figure. Mutation of *pals-22* or *pals-25* does not affect feeding rates of animals**
929 **in pathogen infection assays.**
930 (A,B) Quantification of fluorescent bead accumulation in wild-type, *pals-22*, *pals-22 pals-*
931 *25*, and *eat-2* mutant animals. Beads were mixed with OP50-1 bacteria and either (A) *N.*
932 *parisii* spores or (B) Orsay virus and fed to worms as in infection assays. Worms were
933 fixed in paraformaldehyde after 30 minutes of feeding, and fluorescence of accumulated
934 beads in each animal was measured using a COPAS Biosort machine to measure the
935 mean red signal and length of individual animals, indicated by red dots. Mean signal of
936 the population is indicated by black bars, with error bars as SD. Graph is a compilation of
937 three independent replicates, with at least 100 animals analyzed in each replicate.
938 Statistical analysis was performed using one-way ANOVA. *** $p < 0.001$, ns, not
939 significant.
940
941 **S5 Table. RNA-seq statistics.**
942

943 **S6 Table. FPKM values for all genes in data set.**

944

945 **S7 Table. Differentially expressed genes, as determined by edgeR and limma.**

946

947 **S8 Table. Gene sets used for GSEA and their sources.**

948

949 **S9 Table. Detailed GSEA results.**

950

951 **S10 Table. Gene set overlaps.**

952

953 **S11 Table. Human orthology analysis.**

954

955 **S12 Figure. Induction of *chil-27p::GFP* expression seen after *pals-22* RNAi**

956 **treatment.**

957 Shown are animals treated with either L4440 RNAi control, *pals-22* RNAi, or *M. humicola*

958 infection. The *col-12p::mCherrry* transgene is constitutively expressed in the epidermis.

959 Scale bar, 100 μm.

960

Figure 1

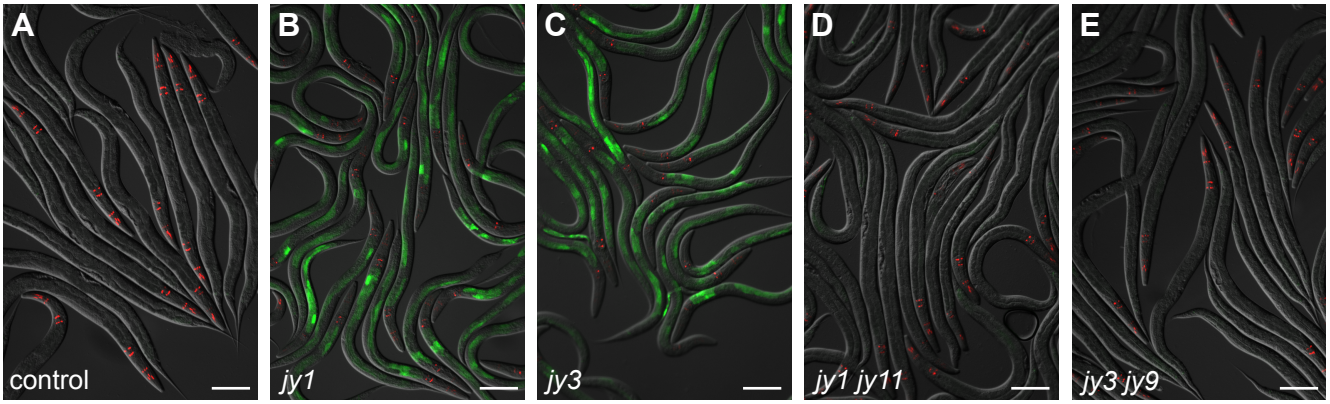
A
control
B
jy1
C
jy3
D
jy1 jy11
E
jy3 jy9

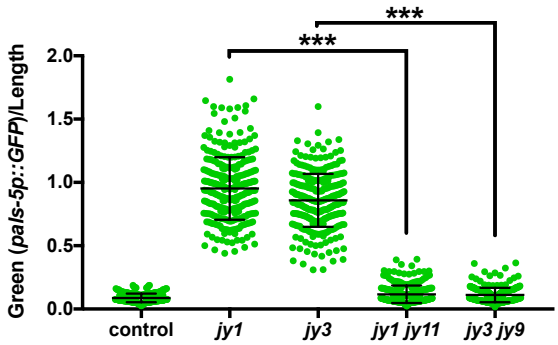
F
Green (pals-5p::GFP)/Length
2.0
1.5
1.0
0.5
0.0
***
***
control
jy1
jy3
jy1 jy11
jy3 jy9

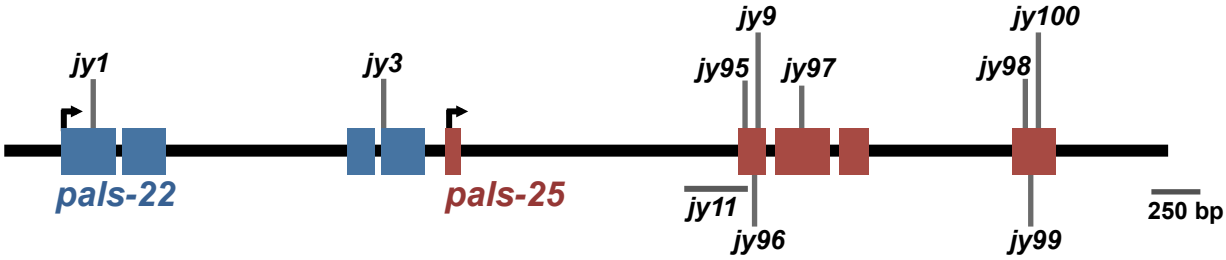
G
jy1
jy3
jy9
jy95
jy97
jy100
jy98
pals-22
pals-25
jy11
jy96
jy99
250 bp

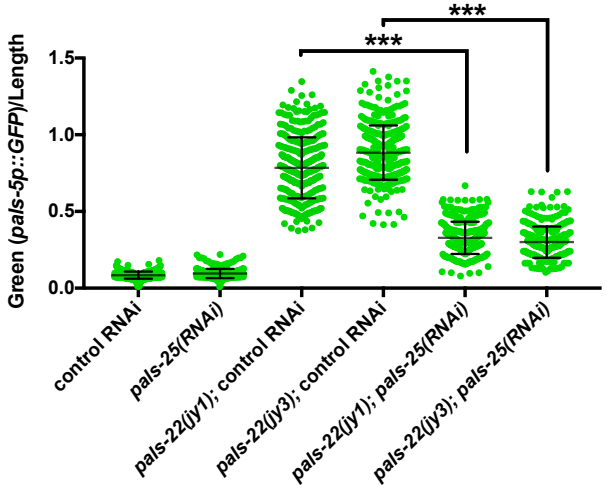
H
Green (pals-5p::GFP)/Length
1.5
1.0
0.5
0.0
***
***
control RNAi
pals-25(RNAi)
pals-22(jy1); control RNAi
pals-22(jy3); control RNAi
pals-22(jy1); pals-25(RNAi)
pals-22(jy3); pals-25(RNAi)

Figure 2

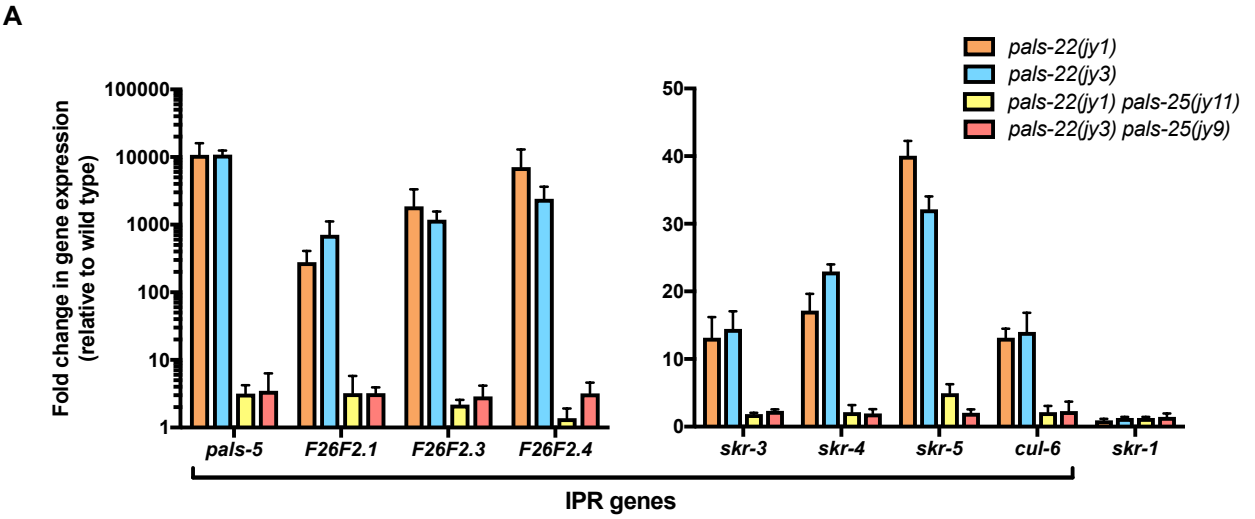
A
pals-22(jy1)
pals-22(jy3)
pals-22(jy1) pals-25(jy11)
pals-22(jy3) pals-25(jy9)
Fold change in gene expression (relative to wild type)
100000
10000
1000
100
10
1
50
40
30
20
10
0
pals-5
F26F2.1
F26F2.3
F26F2.4
skr-3
skr-4
skr-5
cul-6
skr-1
IPR genes

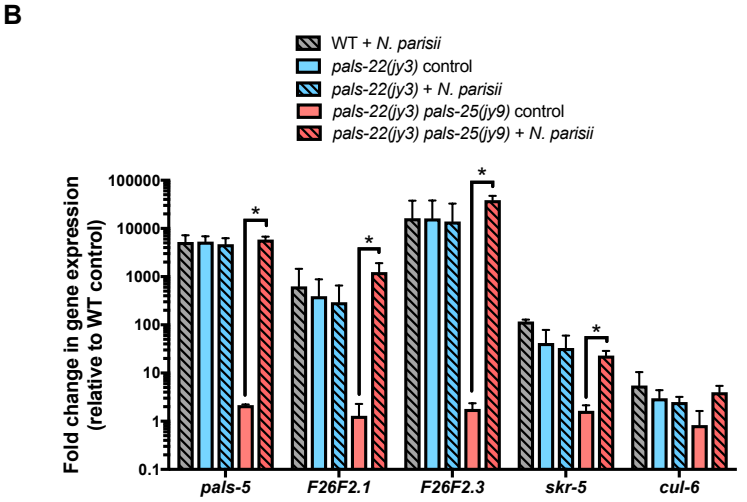
B
WT + N. parisii
pals-22(jy3) control
pals-22(jy3) + N. parisii
pals-22(jy3) pals-25(jy9) control
pals-22(jy3) pals-25(jy9) + N. parisii
Fold change in gene expression (relative to WT control)
100000
10000
1000
100
10
1
0.1
*
pals-5
F26F2.1
F26F2.3
skr-5
cul-6

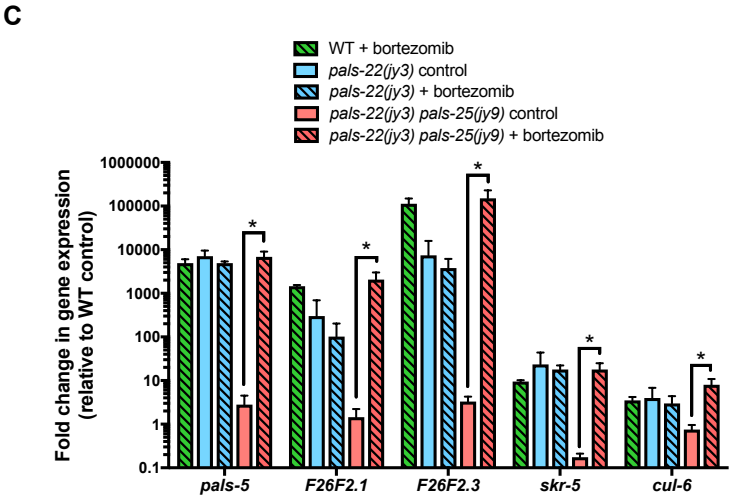
C
WT + bortezomib
pals-22(jy3) control
pals-22(jy3) + bortezomib
pals-22(jy3) pals-25(jy9) control
pals-22(jy3) pals-25(jy9) + bortezomib
Fold change in gene expression (relative to WT control)
1000000
100000
10000
1000
100
10
1
0.1
*
pals-5
F26F2.1
F26F2.3
skr-5
cul-6

Figure 3

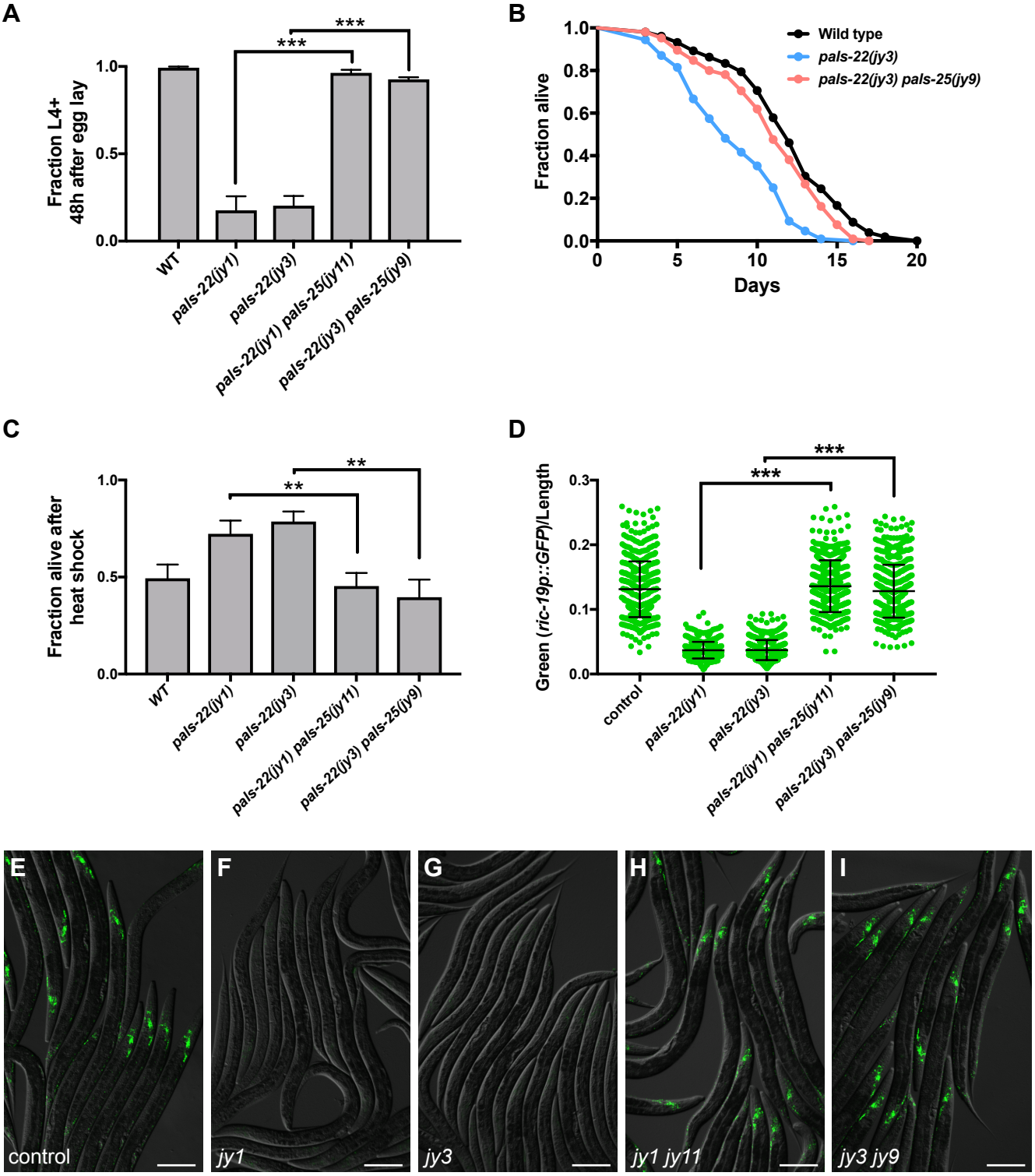
A
Fraction L4+ 48h after egg lay
1.0
0.5
0.0
***
***
WT
pals-22(jy1)
pals-22(jy3)
pals-22(jy1) pals-25(jy11)
pals-22(jy3) pals-25(jy9)
B
Fraction alive
1.0
0.8
0.6
0.4
0.2
0.0
0
5
10
15
20
Days
Wild type
pals-22(jy3)
pals-22(jy3) pals-25(jy9)
C
Fraction alive after heat shock
1.0
0.5
0.0
**
**
WT
pals-22(jy1)
pals-22(jy3)
pals-22(jy1) pals-25(jy11)
pals-22(jy3) pals-25(jy9)
D
Green (ric-19p::GFP)/Length
0.3
0.2
0.1
0.0
***
***
control
pals-22(jy1)
pals-22(jy3)
pals-22(jy1) pals-25(jy11)
pals-22(jy3) pals-25(jy9)
E
control
F
jy1
G
jy3
H
jy1 jy11
I
jy3 jy9

Figure 4

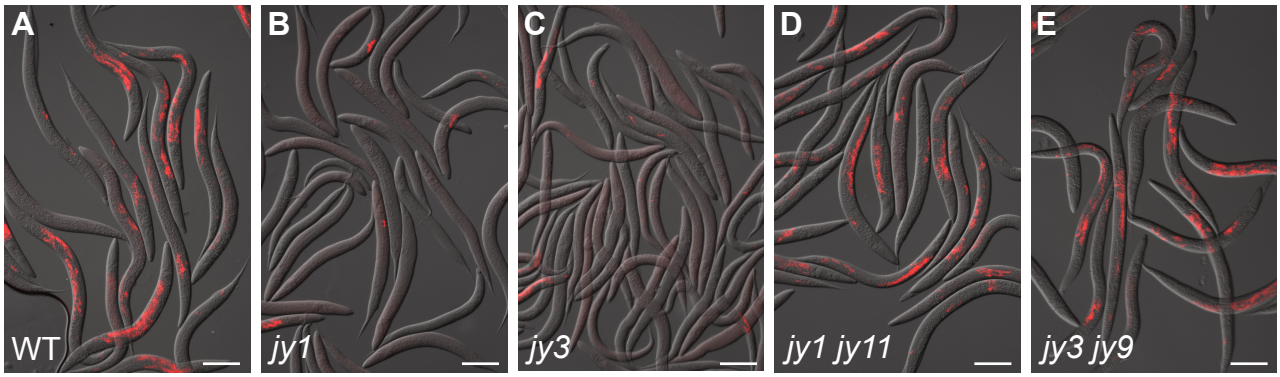
A
WT
B
jy1
C
jy3
D
jy1 jy11
E
jy3 jy9

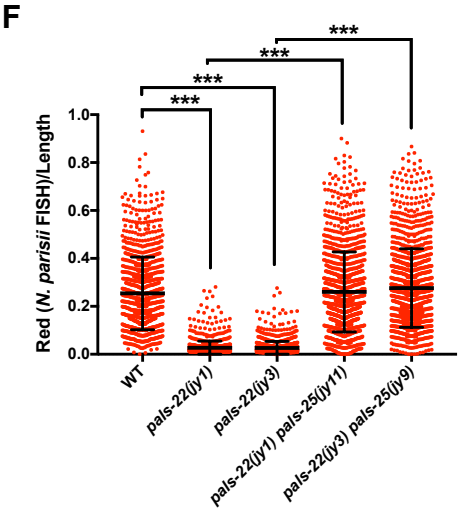
F
Red (N. parisii FISH)/Length
1.0
0.8
0.6
0.4
0.2
0.0
***
***
***
***
WT
pals-22(jy1)
pals-22(jy3)
pals-22(jy1) pals-25(jy11)
pals-22(jy3) pals-25(jy9)

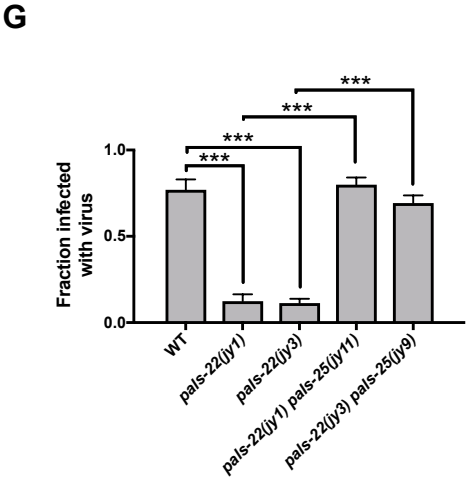
G
Fraction infected with virus
1.0
0.5
0.0
***
***
***
***
WT
pals-22(jy1)
pals-22(jy3)
pals-22(jy1) pals-25(jy11)
pals-22(jy3) pals-25(jy9)

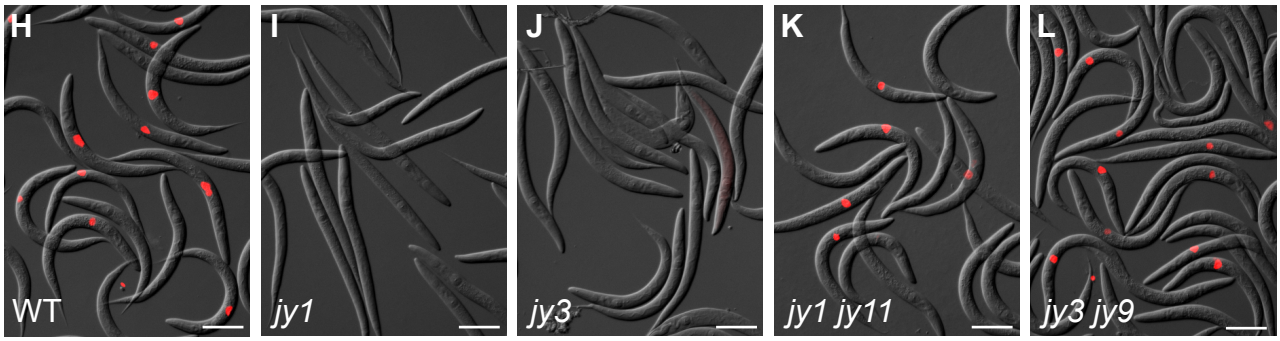
H
WT
I
jy1
J
jy3
K
jy1 jy11
L
jy3 jy9

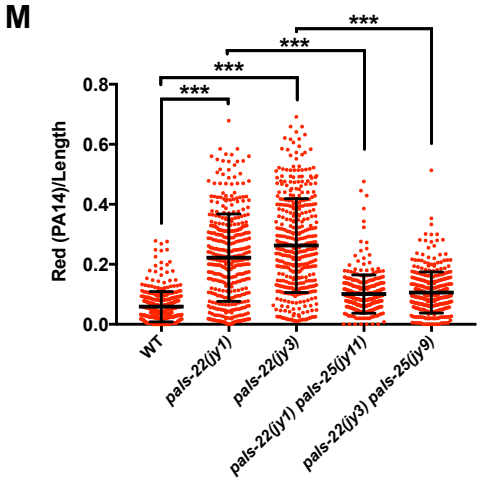
M
Red (PA14)/Length
0.8
0.6
0.4
0.2
0.0
***
***
***
***
WT
pals-22(jy1)
pals-22(jy3)
pals-22(jy1) pals-25(jy11)
pals-22(jy3) pals-25(jy9)

Figure 5

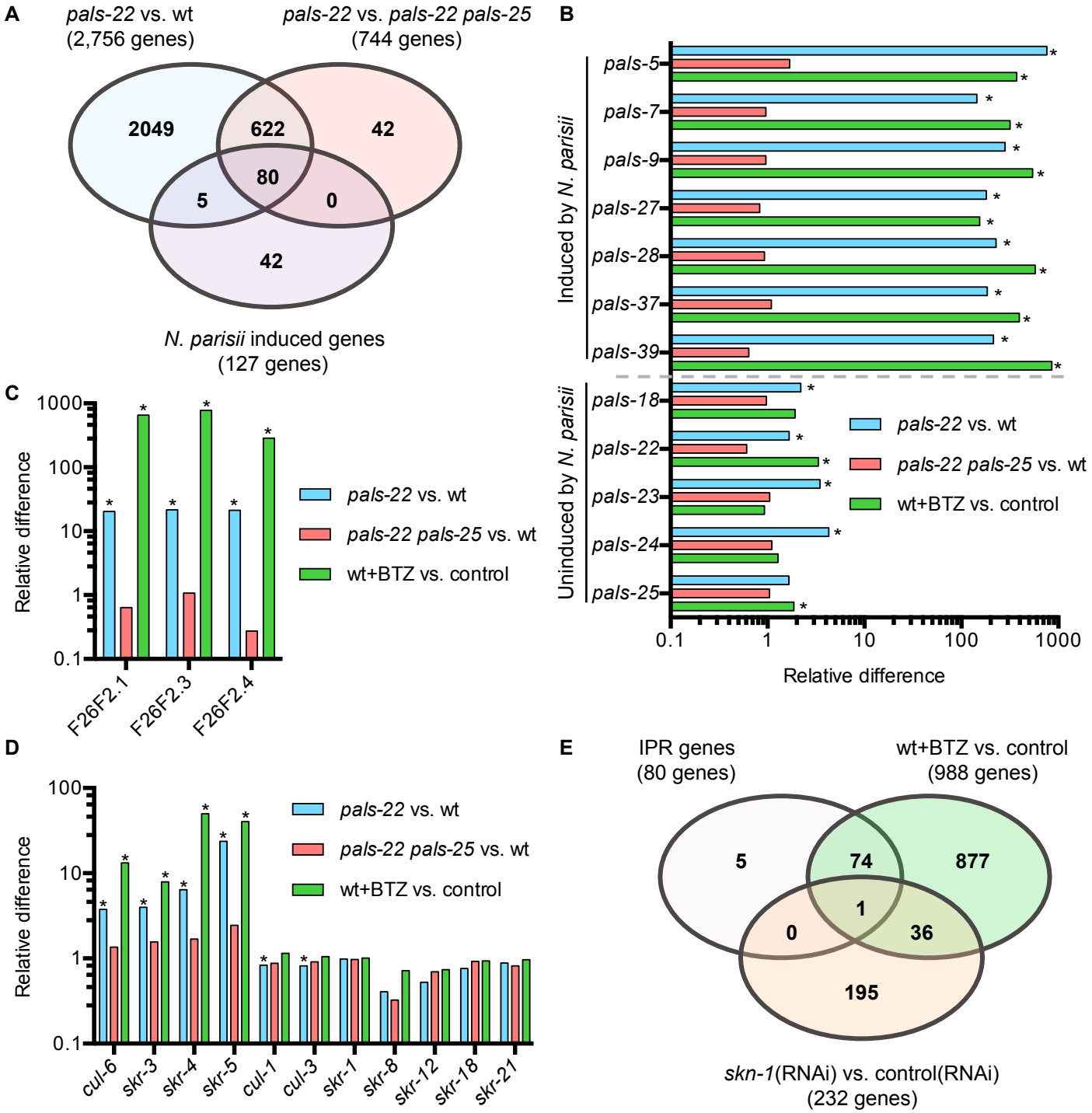
A
pals-22 vs. wt
(2,756 genes)
pals-22 vs. pals-22 pals-25
(744 genes)
2049
622
42
80
5
0
42
N. parisii induced genes
(127 genes)
B
Induced by N. parisii
pals-5
pals-7
pals-9
pals-27
pals-28
pals-37
pals-39
Uninduced by N. parisii
pals-18
pals-22
pals-23
pals-24
pals-25
pals-22 vs. wt
pals-22 pals-25 vs. wt
wt+BTZ vs. control
0.1
1
10
100
1000
Relative difference
C
Relative difference
1000
100
10
1
0.1
F26F2.1
F26F2.3
F26F2.4
pals-22 vs. wt
pals-22 pals-25 vs. wt
wt+BTZ vs. control
D
Relative difference
100
10
1
0.1
cul-6
skr-3
skr-4
skr-5
cul-1
cul-3
skr-1
skr-8
skr-12
skr-18
skr-21
pals-22 vs. wt
pals-22 pals-25 vs. wt
wt+BTZ vs. control
E
IPR genes
(80 genes)
wt+BTZ vs. control
(988 genes)
5
74
877
1
0
36
195
skn-1(RNAi) vs. control(RNAi)
(232 genes)

Figure 6

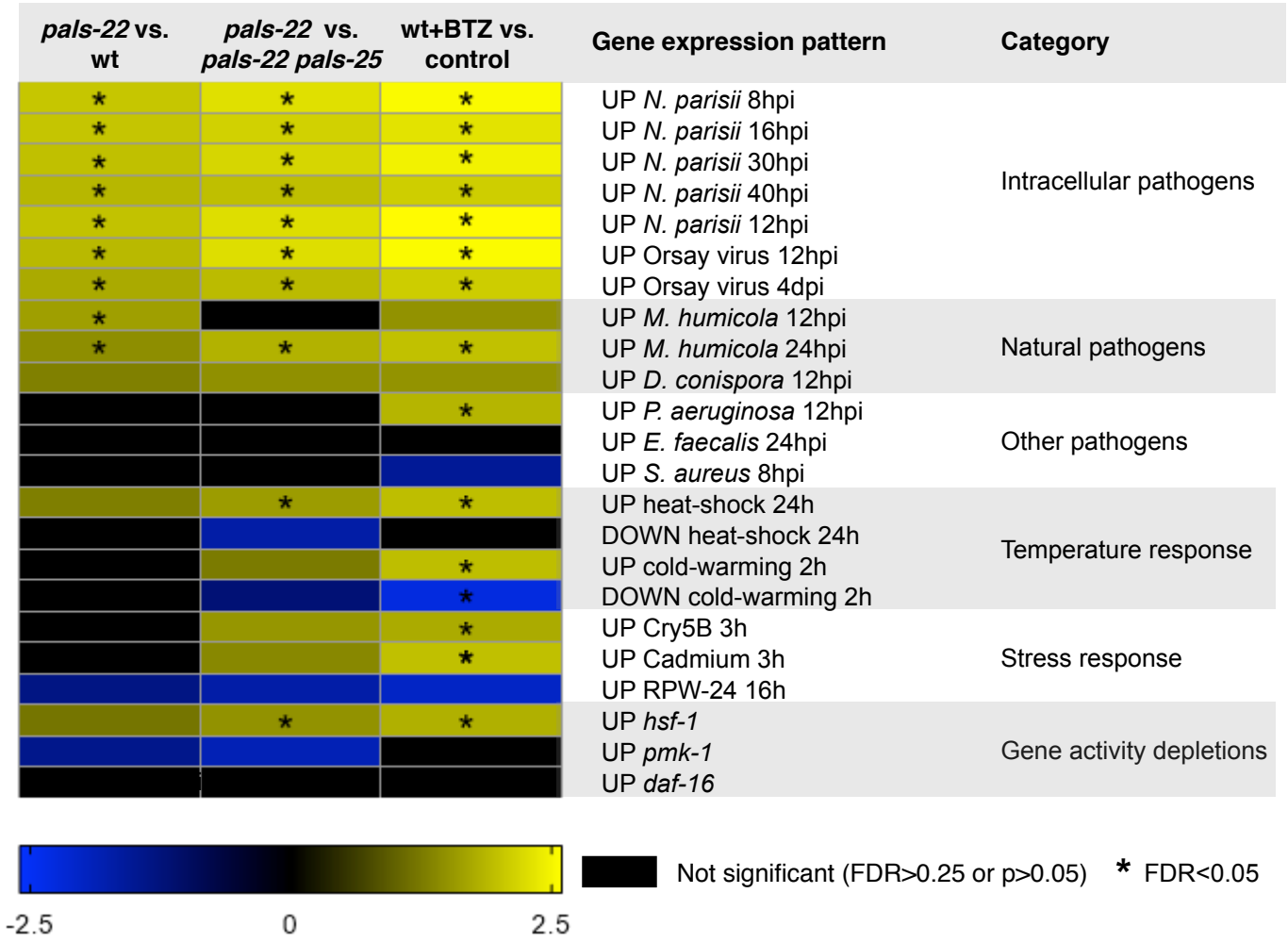
pals-22 vs. wt
pals-22 vs. *pals-22 pals-25*
wt+BTZ vs. control
Gene expression pattern
Category
UP *N. parisii* 8hpi
UP *N. parisii* 16hpi
UP *N. parisii* 30hpi
UP *N. parisii* 40hpi
UP *N. parisii* 12hpi
UP Orsay virus 12hpi
UP Orsay virus 4dpi
Intracellular pathogens
UP *M. humicola* 12hpi
UP *M. humicola* 24hpi
UP *D. conispora* 12hpi
Natural pathogens
UP *P. aeruginosa* 12hpi
UP *E. faecalis* 24hpi
UP *S. aureus* 8hpi
Other pathogens
UP heat-shock 24h
DOWN heat-shock 24h
UP cold-warming 2h
DOWN cold-warming 2h
Temperature response
UP Cry5B 3h
UP Cadmium 3h
UP RPW-24 16h
Stress response
UP *hsf-1*
UP *pmk-1*
UP *daf-16*
Gene activity depletions
-2.5
0
2.5
Not significant (FDR>0.25 or p>0.05)
* FDR<0.05

Figure 7

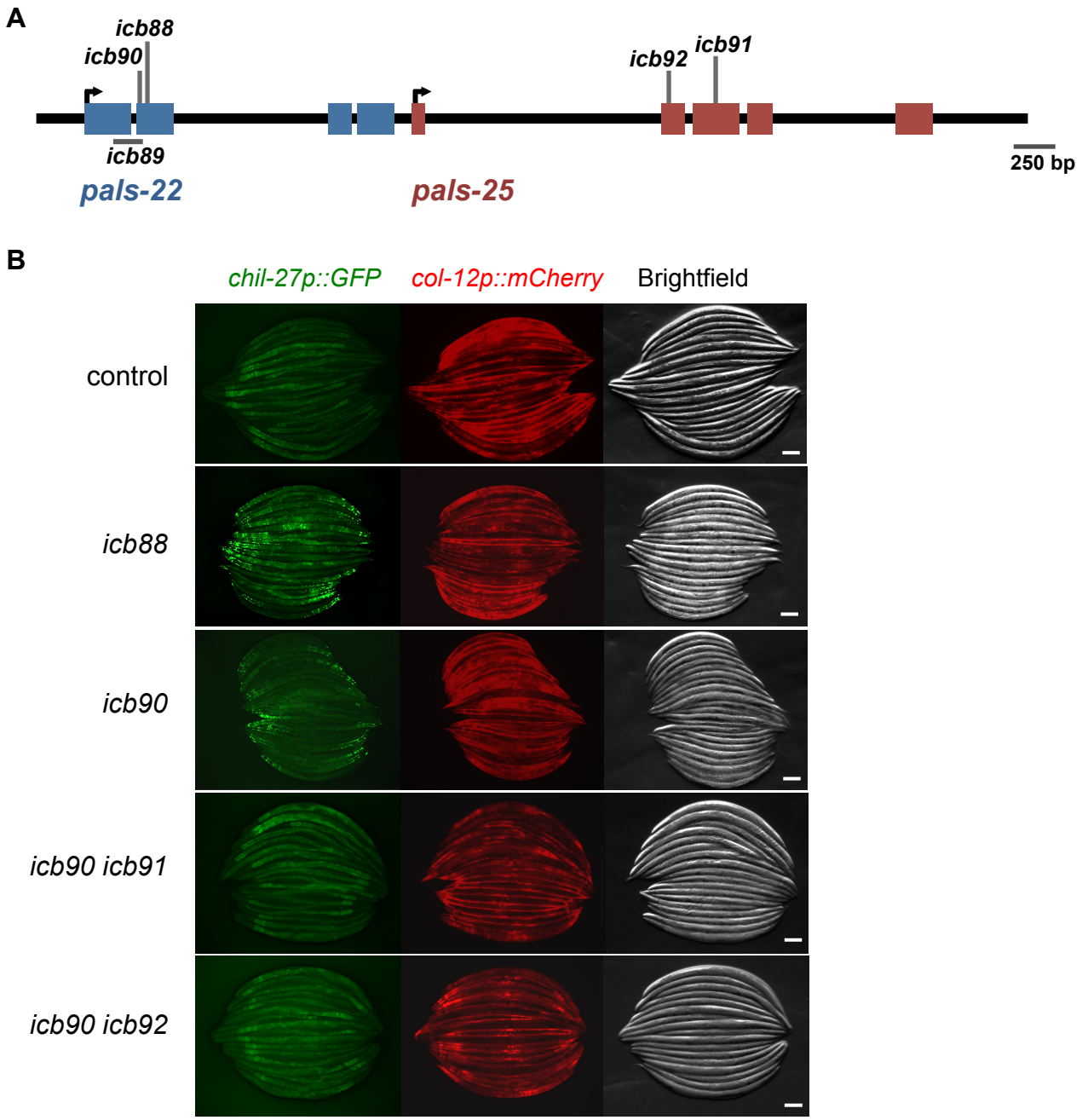
A
icb88
icb90
icb89
pals-22
pals-25
icb92
icb91
250 bp
B
chil-27p::GFP
col-12p::mCherry
Brightfield
control
icb88
icb90
icb90 icb91
icb90 icb92
C
pals-22 vs. wt
pals-22 pals-25 vs. wt
wt+BTZ vs. control
Relative difference
1000
100
10
1
0.1
chil-1
chil-3
chil-4
chil-5
chil-6
chil-9
chil-18
chil-27
chil-28
chil-10
chil-13
chil-14
chil-19
chil-22
chil-23
chil-24
chil-25

Figure 8

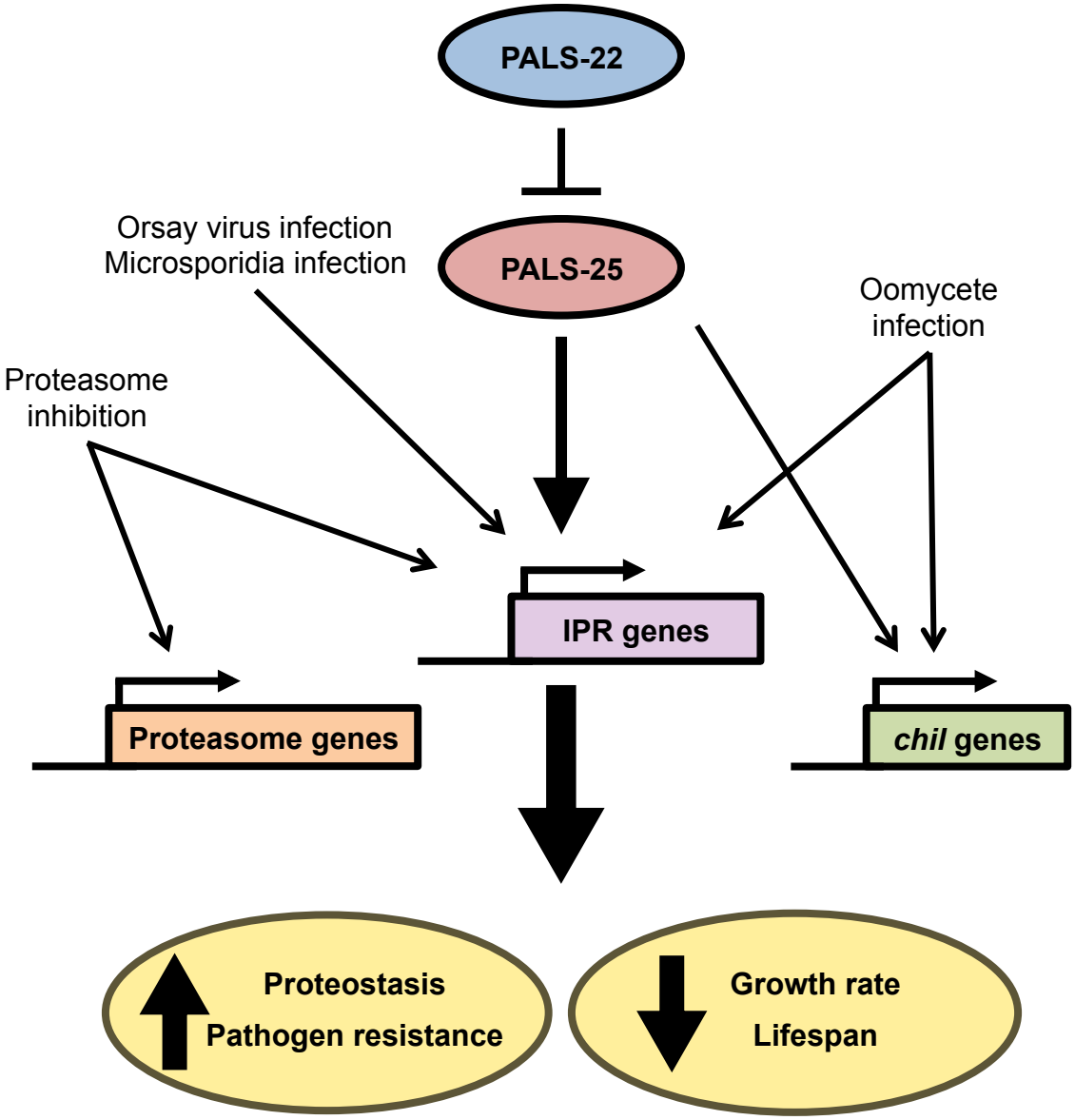
PALS-22
PALS-25
Orsay virus infection
Microsporidia infection
Oomycete infection
Proteasome inhibition
IPR genes
Proteasome genes
chil genes
Proteostasis
Pathogen resistance
Growth rate
Lifespan